Maturing global CO2 storage resources on offshore continental margins to achieve 2DS emissions reductions

GCCC Publication Series #2019-13

P.S. Ringrose
T.A. Meckel

Keywords: characterization, offshore, storage, infrastructure, reservoir, capacity

Cited as:
P.S. Ringrose and Meckel, T.A., 2019, Maturing global CO2 storage resources on offshore continental margins to achieve 2DS emissions reductions, GCCC Publication Series #2019-13, originally published in *Scientific Reports,* 9:17944.

Bureau of Economic Geology
TEXAS Geosciences
Bureau of Economic Geology
Jackson School of Geosciences
The University of Texas at Austin

Maturing global CO_2 storage resources on offshore continental margins to achieve 2DS emissions reductions

P. S. Ringrose[1,2*] and T. A. Meckel[3]

[1] Department of Geoscience and Petroleum, Norwegian University of Science and Technology, Trondheim, Norway
[2] Equinor Research and Technology, Trondheim, Norway
[3] Gulf Coast Carbon Center, Bureau of Economic Geology, The University of Texas at Austin, Austin, Texas, USA
*Corresponding author email phiri@equinor.com

Abstract

Most studies on CO_2 emissions reduction strategies that address the 'two-degree scenario' (2DS) recognize a significant role for CCS. For CCS to be effective, it must be deployed globally on both existing and emerging energy systems. For nations with large-scale emissions, offshore geologic CO_2 storage provides an attractive and efficient long-term strategy. While some nations are already developing CCS projects using offshore CO_2 storage resources, most geographic regions have yet to begin. This paper demonstrates the geologic significance of global continental margins for providing broadly-equitable, geographically-relevant, and high-quality CO_2 storage resources. We then use principles of pore-space utilization and subsurface pressure constraints together with analogs of historic industry well deployment rates to demonstrate how the required storage capacity can be developed as a function of time and technical maturity to enable the global deployment of offshore storage for facilitating 2DS. Our analysis indicates that 10-14 thousand CO_2 injection wells will be needed globally by 2050 to achieve this goal.

(Main Text is 4000 words)

The role of CCS in the energy transition

A major societal challenge is achieving globally significant reductions in greenhouse gas emissions to the atmosphere. There is growing clarity from numerous studies[1,2,3] that large-scale geologic disposal of CO_2 from industrial emissions will be essential to achieve this objective. The 'wedge model' analysis for identifying opportunities for CO_2 atmospheric reductions[4] remains useful for anticipating contributions from different sectors – essentially a blend of growth in renewable energy use, improved energy efficiency, and various means of decarbonization of energy production and consumption. In this construct, CO_2 Capture and Storage (CCS) is anticipated to support approximately 13% of total cumulative emissions reductions through 2050, requiring around 120,000 million tones (Mt) of cumulative CO_2 reduction by 2050. Annual storage rates in 2050 are expected to be 6-7,000 Mtpa[5]. Furthermore, the IPCC argue that emissions reduction costs without CCS deployment could be as much as 29% to 297% higher by 2100[6]. Lastly, many sectors of the modern economy, such as cement and steel production, are dependent on CCS alone to achieve significant decarbonization.

Despite this widespread recognition of the important role of CCS, fundamental doubts seem to remain among communities and policy makers about the viability and effectiveness of CCS deployment. There is certainly a significant economic hurdle, but active projects do exist and costs are decreasing with technology maturation, such that full-chain (capture, transport, storage) CCS can currently be considered as technically demonstrated and available as an integrated decarbonization technology (Norway, Japan, and Brazil have active offshore CO_2 injection projects and the UK, USA, Australia and China have projects in the planning stages).

A recent assessment of the long-term performance and security of CO_2 storage indicates a high degree of confidence in retention[7]. Despite some skepticism about project deployment, there are currently 19 CO_2 injection projects globally[8], of which 4 large-scale projects are dedicated to geologic storage in saline formations (Sleipner, Snøhvit, Quest, IBDP) which together inject nearly 4 million tonnes CO_2 per annum (Mtpa). The 19 large-scale CCS facilities in operation together with a further 4 under construction, have an installed capture capacity of 36 Mtpa[8]. Additional experience in handling, transport, and injection of CO_2 has been gained from almost fifty years of enhanced oil recovery (CO_2

EOR). CCS is therefore demonstrated and underway at industrial scales globally; however, an order of magnitude increase is needed to meet the long-term expectations for CCS and to realize the 2DS goals.

In this paper we reinforce the overall viability of CCS and propose a meaningful timeline by using the historic perspective of the utilization of hydrocarbon resources in sedimentary basins as an analog to demonstrate the future utilization of the same basin geologic resources for CO_2 disposal. Our conclusions offer decision makers a rational perspective for further support to allow CCS to deliver on stated emissions reduction goals. As our focus is on deep subsurface geological storage of captured CO_2 (GCS), we will refer to GCS as the principal objective, assuming that significant global CO_2 capture activities emerge in parallel.

Gigatonne-scale CO_2 storage in offshore basins

Our analysis is based on the broad similarities in the stratigraphic and tectonic histories of passive continental margins and clarifies the primary factors affecting basin-wide and global storage potential (capacity), emphasizing typical subsurface fluid pressure profiles. Important local and regional differences in the tectonic histories of the continental margins are discussed in the supporting methods paper[9]. Our approach departs from extensive prior regional volumetric quantification techniques[10] that rely on a subsurface volumetric efficiency factor (ε). Rather, we develop concepts that emphasize regional stratigraphic pressure constraints that will matter at the Gigatonne (Gt) storage scale, referred to here as the 'basin ΔP' approach. We then demonstrate, using historic industry hydrocarbon well development data at three different regional scales, combined with rational average injection rates informed by the stratigraphic pressure analysis and practical experience, that accessing this storage resource is possible on the required timeframes and within pressure constraints that allow GCS to deliver the expected emissions mitigation role. We also argue that the history of technology development in extracting oil and gas resources over the last century (termed the primary, secondary and tertiary recovery methods) can to some extent be applied for evaluating similar future phases of CO_2 disposal technology, each employing more advanced pressure management methods. Our aim is to provide the first-order technical basis and confidence that various nations need to effectively and simultaneously develop their offshore geology for GCS on a timeline that is relevant for 2DS[11].

The global offshore continental shelves (Fig. 1) represent the most significant Gt-scale storage resource for GCS. Onshore basins are also important, but the offshore settings offer both significant volumes and practical deployment benefits at scale. Offshore continental margins, dominated by thick Cenozoic-age sediments provide vast subsurface rock volumes broadly prospective for storage due to their suitable subsurface depth range and relatively young age (low compaction, limited diagenesis, and high porosity). This volumetrically-significant resource can adequately and efficiently match the global objective of Gt-scale CO_2 disposal. Furthermore, this resource benefits from lower technical and societal risks related to regionally-limited access to suitable onshore geology (e.g. EU, Atlantic US, China and India), issues related to protection of potable groundwater resources, and avoidance of population centers. The existence and historic exploitation of numerous giant hydrocarbon accumulations in offshore basin settings (Fig. 1, yellow symbols) can also be taken as evidence for appropriate subsurface conditions for retention of large volumes of buoyant non-wetting fluids over geologic time scales, giving an excellent precedent for successful deployment of GCS. Regional comparison of the overall similarity of geographic extent of available storage resources for select regions is provided in Figure 2, illustrating a broadly equitable storage and geographically relevant resource potential.

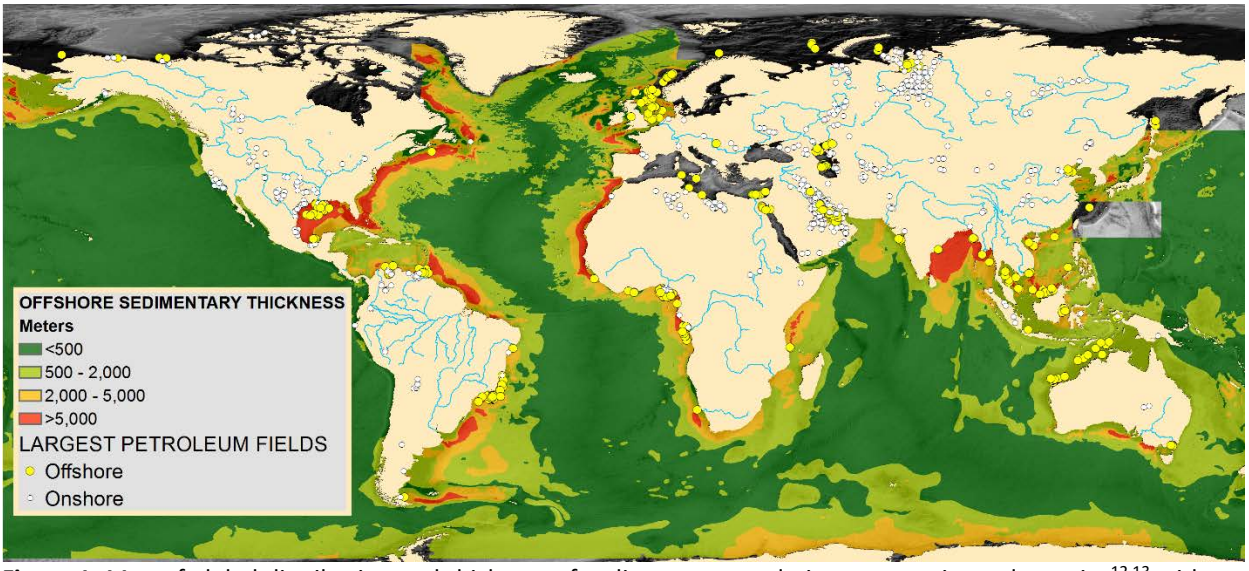

Figure 1. Map of global distribution and thickness of sediment accumulations on continental margins[12,13] with the thickest stratigraphy indicated in red. Yellow dots represent the largest offshore hydrocarbon fields (i.e. suitable large-scale subsurface hydrocarbon containment demonstrated[14], and blue lines are the largest continental river systems, often leading to extensive and thick offshore Cenozoic stratigraphy.

Many offshore continental margin basins (Figs 1 and 2) have comparable geologic evolution that has resulted in broadly similar stratigraphic and structural elements: typically, a phase of continental rifting and subsidence followed by a period of passive margin coastal progradation[15,16]. Decades of investigation indicate that these margins exhibit a deeper rift sequence with some variability in structural style[17], typically Mesozoic in age (often representing the rifting of the Pangaea supercontinent around 175 million years ago), with advanced diagenesis (cementation and porosity reduction due to burial and interaction with hot fluids). These deeper rift sequences are typically overlain by net-progradational and aggradational Cenozoic sediments composed of fluvial, deltaic, shelf, and slope deposits. Where large continental-draining river systems enter these settings (Fig. 1, blue lines), clastic accumulations may exceed many kilometers thickness. Other margins may have extensive carbonate development[18], also suitable for GCS. These Cenozoic-age passive margin deposits are also characterized by lower levels of diagenesis (porosity reduction) and less pervasive faulting than the underlying Mesozoic stratigraphy. Arguably, the deeper rift sequences are less well-suited for the first phase of GCS, while the upper Cenozoic sequences offer some of the best regional saline aquifer storage targets (such as the Utsira sandstone offshore Norway; Fig. 2). In all cases, the essential storage requirement is to find thick high-porosity sediment reservoir units overlain by sealing units (usually thick shales), ideally with open hydrologic systems for dissipating induced pressure increases. Shallower projects also have reduced drilling costs. The deeper rift sequence often includes many large-scale faults that often propagate upwards and generate additional subsequent faulting in the overlying stratigraphy. The fault architecture is also a critical element for storage site characterization, since faults can both transmit and retain buoyant fluids[19,20]. In a global petroleum assessment, 71% of the known hydrocarbon reserves occurred in structural (i.e. faulted) traps, as opposed to stratigraphic or other trap types[21], suggesting faults are commonly involved in high-saturation subsurface buoyant fluid retention.

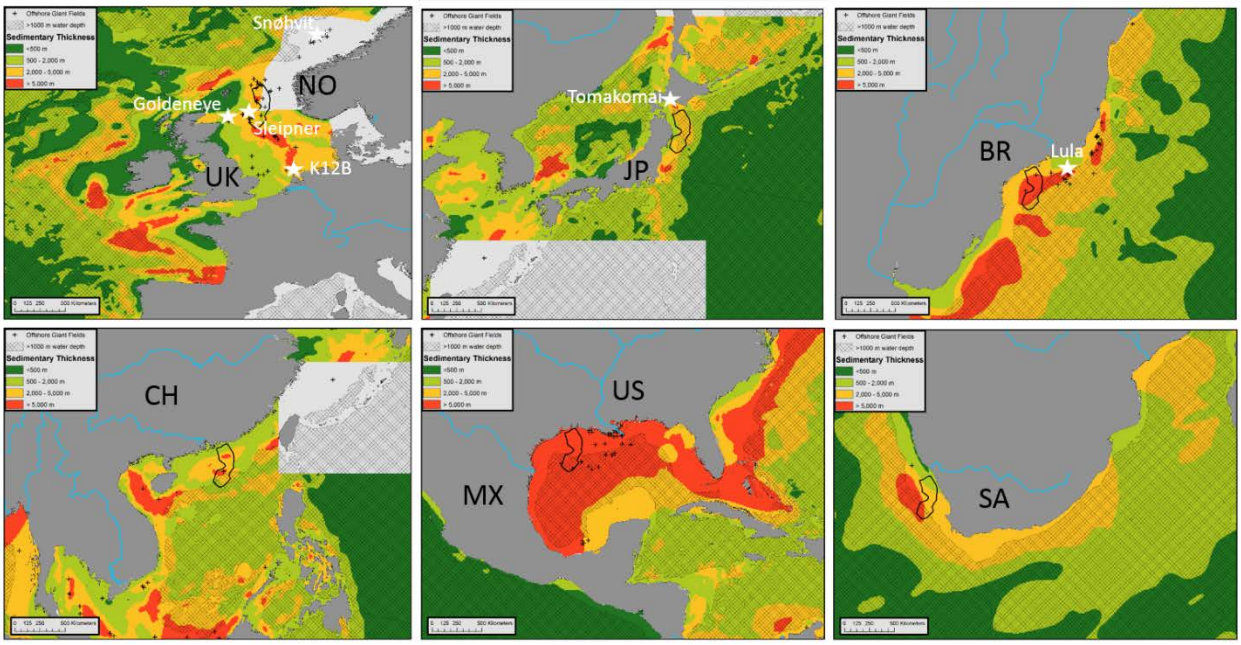

Figure 2. Comparison of prospective storage resource regions for selected global localities at the same map scale (1:15,000,000). The footprint of the Utsira sandstone formation (North Sea) utilized for GCS since 1996 is indicated in the solid black outline and represents the size of a typical regional geologic storage target. Currently active (Sleipner, Snøhvit, Tomakomai, Lula), completed (K12B) and proposed (Goldeneye) offshore CO_2 injection projects are indicated with white stars. Cross-hatched regions have water depths >1,000 m. Major hydrocarbon fields (Fig. 1) are shown in black cross symbols, indicating favorable conditions for large-scale subsurface retention of buoyant fluids.

Basin-fluid pressure analysis approach

Two of the three largest global hydrocarbon (oil and gas) producing regions are the North Sea and the Gulf of Mexico – the largest being the Middle East/Persian Gulf region, which is mainly onshore and partly offshore. We will therefore consider these two basins as representative of a mature state of subsurface knowledge for the highly prospective offshore basins available for large-scale CO_2 disposal. One of the most significant common features in geologic development of the continental margins is the subsurface fluid pressure distribution[22]. Typically, these geologic basins have a shallow interval (<2-3 km) with hydrostatic (normal) pressures that develop with depth into naturally over-pressured systems, a common feature which can be deduced from the initial reservoir pressure data from decades of hydrocarbon exploration in different basins[23,24,25,26,27]. This behaviour is essentially controlled by a natural balance between the rate of compaction and the rate of fluid pressure dissipation[28], where a loss of balance is usually termed 'disequilibrium compaction', although other processes are also involved in generating overpressure[29].

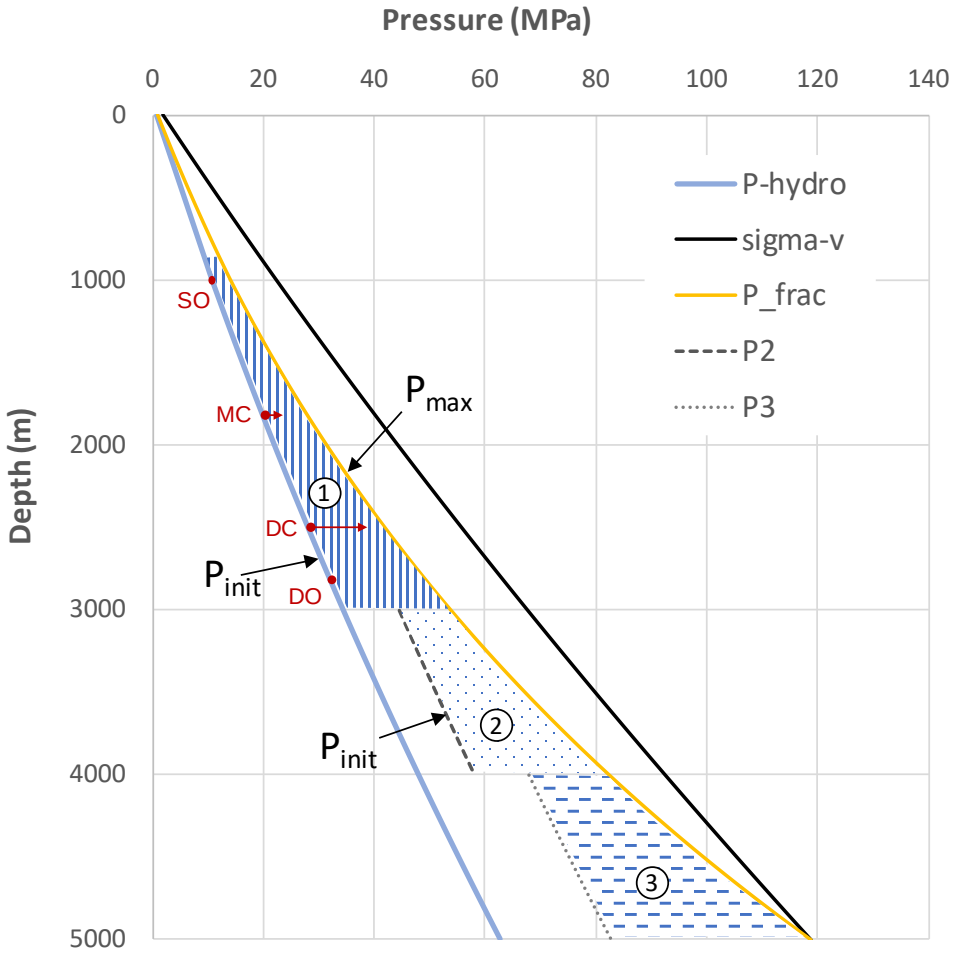

Figure 3. Pressure depth functions for a generalised Norwegian North Sea basin case illustrating the shallow normally pressured region (1), and the progressively deeper and more overpressured regions (with excess initial pressure P2 and P3). P-hydro is the hydrostatic gradient, sigma-V is the vertical principal stress, and the maximum reservoir pressure is described by the formation fracture pressure P_frac (see methods paper[9]).

As the fluid pressure increases with depth it begins to approach the lithostatic pressure gradient, and a limiting pressure is reached – the rock fracture pressure – such that subsurface reservoirs rarely exhibit pressures greater than 80-90% of the lithostatic pressure (often taken to be 22.6 kPa/m or 1 psi/ft). This general behavior is characterized in the depth plot shown in Figure 3, based on a generalized Norwegian North Sea basin case. For comparison, average initial-reservoir pressure trends for all Miocene reservoirs on the inner shelf of Texas[30] are shown to be hydrostatic to approximately 2,750 meters[31], consistent with regional GoM data[32]. Three depth zones are identified in this generic plot: (1) a normally pressured zone between 1 and 3 km depth, (2) a weakly over-pressured zone between 3 and 4 km depth, and (3) a high over-pressured zone between 4 and 5 km depth. The actual depths of these zones and style of vertical transition will be basin dependent, but the trend with depth is commonly observed. Referring to the stratigraphic summary above, the Cenozoic sequences are typically in the normally-pressured zone, while the deeper Mesozoic rift-sequences are commonly found in the deeper over-pressured zones (with many exceptions to that simplification).

Appreciation of this common fluid pressure trend with depth (Fig. 3) is arguably the single most significant consideration for offshore global GCS deployment at the Gt-scale in a reasonable timeframe (assuming that the basic reservoir and seal characteristics are identified[33]). This is because large-scale CO_2 disposal will require subsurface pressure management, rather than being simply controlled by the available subsurface pore volumes. While pore volume is a static metric, pressure evolution involves

time, which is an important consideration for understanding how GCS can meet intended volumetric targets within anticipated timelines through mid-century. This has been described as 'dynamic capacity' [34], and while pressure constraints have been identified and discussed previously as key factors for CCS[35,36,37,38], this evaluation has primarily been considered for reservoir-scale performance[39] rather than at a stratigraphic scale.

Reservoir pressure mitigation methods involving subsurface brine extraction have also been investigated[40], but ultimately include re-injection into another nearby stratigraphic interval, which does not overcome the large-scale stratigraphic pressure limitations that are considered here. So, while brine extraction and re-injection may enable single projects to be optimized, the strategy is not necessarily favorable for long-term Gt-scale storage in a basin employing multiple projects throughout the stratigraphy and may not be required. However, pressure management among multiple projects may be useful in the later stages of storage resource development (as argued below).

Thus, while CO_2 storage trapping mechanisms[41] (structural trapping, residual-phase trapping, dissolution and mineralization) are essential to GCS, it is the subsurface reservoir pressure that ultimately limits CO_2 injection and the total storage capacity at the Gt-scale at operational timescales. Pressure propagates in the subsurface far more effectively and pervasively than injected fluids, and the pressure footprint can be assumed to extend outward from an injection well by a factor of 10 to 100 compared to the dimensions of the CO_2 plume[42]. The importance of pressure limitations was encountered at the Snøhvit project in the Barents Sea (a Mesozoic injection target), where the initial injection well had to be modified to allow access to stratigraphic units with better pressure communication[43,44]. As a corollary, the Sleipner project (Cenozoic) has not encountered any pressure limitations, being connected to a large open aquifer system. Here, we develop the concept of the 'available pressure resource' for global deployment of offshore GCS, using the cases of the North Sea and the Gulf of Mexico as a reference.

Our proposed generic approach, the 'basin ΔP' approach, is based on integration of the injectivity equation over the project lifetime, where pressure limits are defined by basin pressure. We obtain the following function (see supporting methods paper[9]):

$$V_{project} = I_C \left[p_{well} - p_{init} + \int_i^f A\, p_D(t_D) \right] + F_b \qquad (1)$$

where,
$V_{project}$ is the estimated volume stored
I_c is the injectivity
P_{well} is the injection well pressure
P_{init} is the initial reservoir pressure
$Ap_D(t_D)$ is a characteristic pressure function
F_b is a volume flux boundary condition

The characteristic pressure function, the integral of reservoir pressure with time, is a function of the formation properties and the dimensions of the storage unit, represented graphically in Figure 4. The integration is between the limits P_{init} and P_{final}, where P_{final} may be defined with reference to p_{frac} as a limiting condition. For a closed saline aquifer unit with no-flow boundary conditions (such as a sealed fault block), $F_b = 0$; while for the case of some pressure dissipation from the saline aquifer formation, F_b is positive, and for a case with some brine influx into the storage unit F_b is negative. It is generally assumed that F_b is a small factor compared to the injectivity term. However, for the case of an infinite aquifer with no pressure boundary limitation, F_b could be large or even dominant.

Equation (1) assumes a constant injection pressure and constant injectivity – simplifying assumptions appropriate for screening prospective projects and evaluating expected GCS performance. With more complex operational variables, numerical reservoir simulation can be used to more accurately assess injection volumes as a function of variable pressure gradients. At the project screening stage, parameters for equation (1) can be estimated using regional basin data[9] and initial

estimates of storage unit geometry and formation permeability. Volumes may be converted to mass using estimates for the mean *in situ* CO_2 density. An illustration of the application of equation (1) to a real dataset is also given in the methods paper[9].

There are essentially two operational criteria for stopping storage projects:

A. The storage project fills the available pore-space before the maximum pressure limit is reached (Aquifer geometry A in Fig. 4);
B. The storage project reaches the maximum pressure limit before the available pore-space can be fully utilized (Aquifer geometry B in Fig. 4).

The concept outlined in Fig. 4 is scaled to a common set of initial conditions: the initial reservoir pressure, P_{init}, the bottom-hole well pressure, P_{well}, and the formation fracture pressure P_{frac}. Storage geometry A follows a pressure path P_a towards a final pressure P_{fa}, and likewise for B.

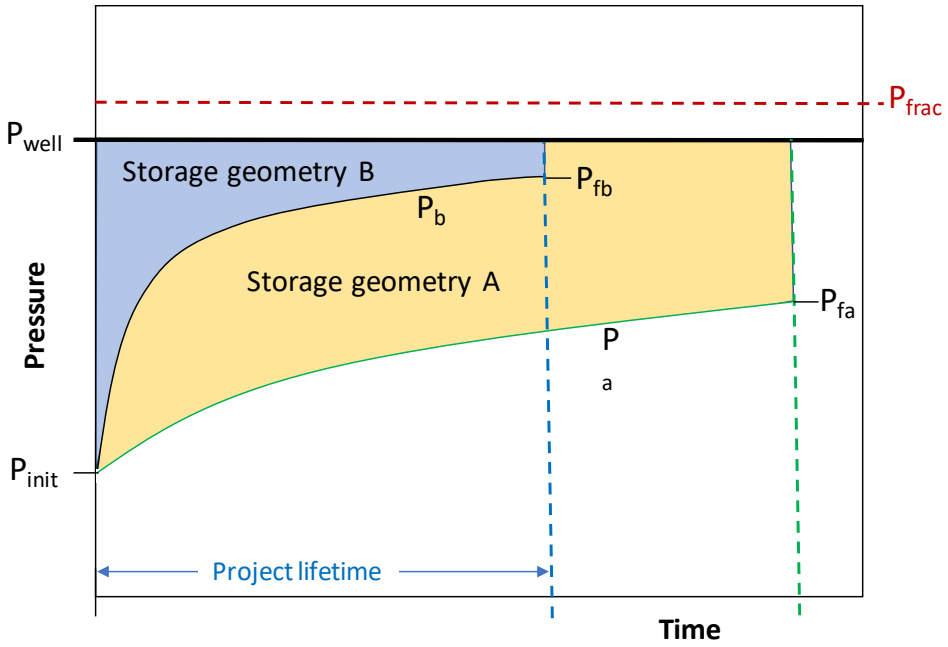

Figure 4. Idealised project lifetime pressure plots for two contrasting aquifer units assuming the same initial pressure conditions.

The Sleipner and Quest projects are examples of A, while the early injection history at the Snøhvit project was an example of B. A further situation is also possible where CO_2 is injected in an inclined aquifer, with lateral migration gradually being hindered and eventually stopped by processes of structural, residual and solubility trapping[45,46]. This would be a variant of A, since pressure would not be a limiting factor.

Thus, in general, if all prospective storage formations fall into either of these two categories, the total storage resources will be smaller than the initial static volumetric estimates based on storage efficiency, ε, since the B-category aquifers will be pressure limited. As we argue below, early projects will tend to focus on the best available storage opportunities provided by 'Class A' aquifers (and in the offshore basins these will typically be found in the shallower mainly post-rift Cenozoic stratigraphy). As the global need to access storage resources grows, projects will then start to exploit the 'Class B' aquifers, having to adjust project designs to cope with the local formation pressure limits. A third class of storage projects, which we will term 'Class C' will be the cases where active pressure management is used to further enhance storage availability. This will allow natural pressure limits to be circumvented by active production schemes, including brine production[47] the use of the 'pressure space' created by oil and gas production[48] or direct injection into depleted gas fields[49]. We argue that this transition from early use of CO_2 injection into aquifers without significant pressure limits (Class A), through to CO_2 storage in pressure-limited aquifers (Class B) and eventually to pressure

management at the basin scale (Class C), represents a global technology development strategy for storage (Table 1), which is analogous to the historic oil and gas production strategy which has moved from primary recovery (pressure depletion modus), to secondary recovery technology (mainly pressure management by water injection), and then to tertiary methods (involving injection of gas, CO_2 and other chemicals to further enhance hydrocarbon recovery). We know from historic data that each new phase of oilfield recovery added a factor of 0.5-1 to the previously recoverable oil resources.

Oil and gas domain	**Primary production**	**Secondary recovery**	**Tertiary recovery**
Recovery mechanisms used	Pressure depletion	Pressure support (mainly waterflood)	Gas & CO_2 injection, chemical flooding
Typical recovery factor (% HCIP)	< 30 %	30 to 50 %	40 to 80 %
CO_2 storage domain	**Class-A projects**	**Class-B projects**	**Class-C projects**
Pressure management approach	Projects with minimal pressure constraints	Projects constrained by pressure limits	Projects with active pressure management
Typical pore space utilized (% Pore Volume)	<6% of open aquifer systems	<4% of confined aquifer systems	>5% for targeted confined aquifer systems

Table 1. Comparison of historic oil and gas recovery strategies with the proposed CO_2 storage resource.

It is not simple to predict how successive stages of technology development will work to increase the accessible CO_2 storage resources, but as an indicator of this potential we can use the relatively mature storage resource assessments for the Utsira formation offshore Norway[50]. For the Utsira Fm. structural trapping of free-phase CO_2 (a Class-A resource) provides ~0.8 Gt of storage[51], while injection up to the natural pressure limits (Class-B resource) could allow up to 8.3 Gt of storage[52]. Studies of the potential Utsira storage resource when deploying active pressure management (Class-C resource) gave estimates between 42 and 50 Gt of storage[51,53]. The potential for growth in storage resources as a function of increasing application of technology is therefore significant. This strategy for utilization of the global offshore basin storage resource is captured graphically in Figure 5.

To illustrate the range of likely behaviour of different CO_2 injection projects at different stratigraphic depths and contrasting reservoir conditions, we postulate four model scenarios (also shown on Fig. 3):

a) A shallow open-boundary case (SO) with injection at 1000m depth and with no significant pressure constraint (a Cenozoic Class-A resource);
b) A moderate-depth, partially-closed pressure boundary case (MC) with injection at 1800m depth (a Cenozoic Class-B resource);
c) A deep closed-boundary case (DC) with injection at 2500m depth (a Mesozoic Class-B resource);
d) A deep open-boundary case (DO) with injection at 2800m depth and with no significant pressure constraint (a Mesozoic Class-A resource).

These have been modeled using equation (1) to estimate the storage metrics and have well rates that cover the observed range in historical injection data[9]. Of course, a wide range of scenarios are possible – these are only intended to portray representative well behaviors. Of these 4 scenarios, the DC case reaches a pressure limit before the end of the expected well life of 25 years, resulting in only 5.1 Mt stored at project closure in year 16. The best case (SO) achieves 23.4 Mt stored after 25 years, and the mean injection rate for all four cases is 0.57 Mtpa, close to the historical mean of 0.53 Mtpa and lower than the historical mean for offshore wells at 0.7 Mtpa.[9]

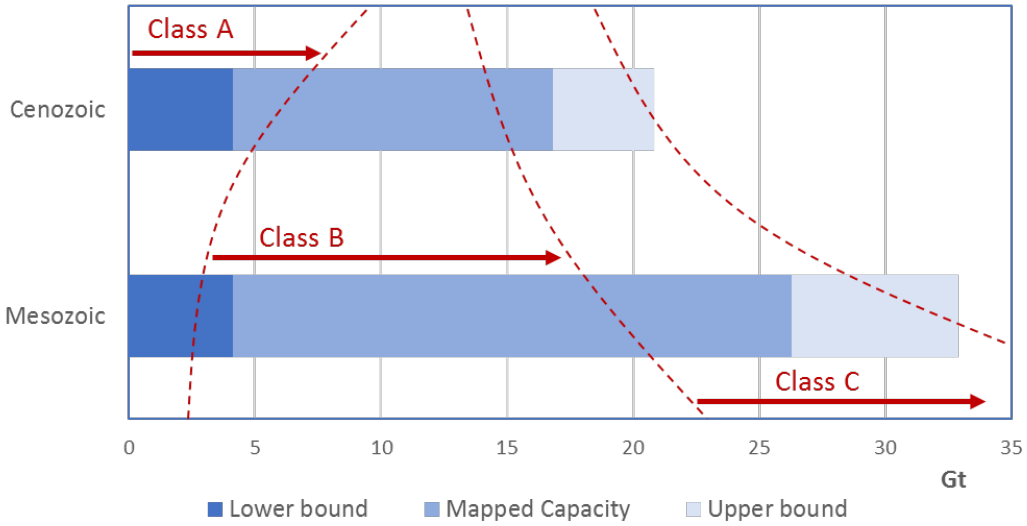

Figure 5. CO_2 storage resource development strategy, illustrated for the case of the mapped Norwegian North Sea resource base. Here we have used the lower-bound resource estimate to identify the Class A resource with a preference for initial deployment in the shallower Cenozoic stratigraphy. Class B approaches the mapped capacity values and utilizes deeper stratigraphy. Class C is used to exploit the upper bound potential in the last phase.

Parameter	**SO**	**MC**	**DC**	**DO**
Injection Depth (m)	1000	1800	2500	2800
Formation Temperature (C)	35	63	88	98
P initial (bar)	108.0	200.0	290.0	319.0
P final (bar)	110.0	230.2	390.7	323.0
P well (bar)	138.0	250.0	380.0	380.0
Injectivity (m3/day/bar)	120	80	40	30
Pressure constraint factor, A	1	15	50	2
Mean annual injection rate (Mt)	0.9	0.7	0.3	0.4
Total injected (Mt)	23.4	9.2	5.1	11.4
Project termination year	25	25	16	25

Table 2. Parameter assumptions for four injection-well model scenarios and resulting storage metrics. Volume to mass conversion uses standard properties for CO_2 assuming thermal equilibrium. The average annual injection rate across the four cases is 0.57 Mtpa.

Global CO_2 injection development well rate and timeline

Given the reservoir performance concepts developed above, and the constraint of expected average injection rates, how then could a strategy for systematic use of this subsurface offshore continental margin stratigraphic storage resource be implemented? We address this by considering the history of hydrocarbon industry development in the selected regions to provide a template for a credible deployment timescale for CCS as an analog for achieving global emissions reduction targets.

Figure 6 presents future well-development based on historical well performance for the Texas inner shelf of the Gulf of Mexico, the entire Gulf of Mexico, and the Norwegian North Sea (well count data from Texas Railroad Commission, U.S. Bureau of Safety and Environmental Enforcement, and the Norwegian Petroleum Directorate). The primary data provided are the annual and total cumulative

number of wells drilled in each region. The historical curves have each been shifted such that the initial year for the first well is 2020 (although a few offshore CO_2 injection wells existed globally before that time). The cumulative number of historic hydrocarbon wells has been translated to storage volumes assuming a 25-year well life for each CO_2 injection well, a reasonable assumption given the experience with enhanced oil recovery using CO_2 injection wells in the Permian Basin of west Texas. This results in some fall-off of active well numbers in the years after 2050, most noticeably in the Gulf of Mexico dataset. The number of wells active in 2050 in these scenarios are 17,155 for the Gulf of Mexico case, 2,083 for Norway and 345 for Texas.

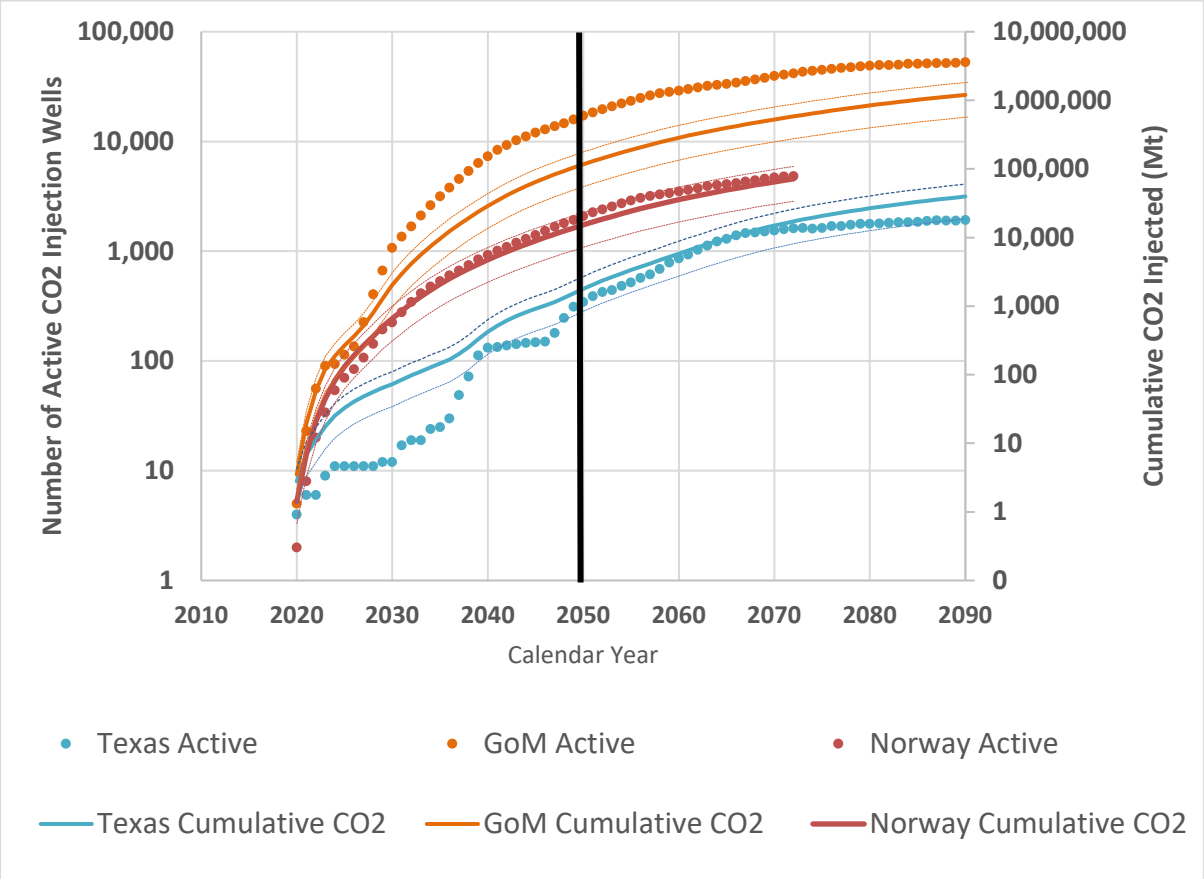

Figure 6. Projected growth of the number of CO_2 injection wells and the cumulative CO_2 injected, based on historical hydrocarbon well development for three different geologic regions. Historic datasets have been replotted beginning in 2020 to provide a perspective on potential future regional CCS well deployment. The lower slope of the data in late years is a result of hydrocarbon production maturation (resource depletion, creaming concepts), which might also occur with CO_2 storage when resource limits are eventually reached (volume or pressure). Thin dashed lines represent high (P10) and low (P90) bounds[9] based on injection rates of 0.33 and 1.06 Mta.

The mean CO_2 injection rate per well is assumed to be 0.7 Mtpa (or 17.5Mt per well over the 25-year lifetime), based on the available data for injection rates to date[9] and consistent with pressure-sensitive results derived in Table 2. Using available historic data from industrial-scale storage projects in operation[9] we obtain rate estimates of 0.532±0.271 Mtpa for all wells and 0.695±0.222 Mtpa for the offshore wells only. Using the offshore wells statistics[9] we then obtained values for a 90% confidence interval: P90=0.33, P50=0.70, P10=1.06 (where P90 indicates 90% probability of exceedance). We recall that the IEA[5] envision global CCS deployment capable of capturing and storing up to 7 Gt of CO_2 emissions per year in 2050, with total cumulative mitigation of 120 Gt at that time[54]. Using the assumed mean injection rate of 0.7 Mtpa per well, this implies that over 10,000 CO_2 injection wells (delivering 7,000 Mt per year total) may need to be in operation by 2050. Is this plausible? Essentially yes, considering historic well development rates. For example, by converting the historical

well development trajectories into future CO_2 injection wells (Fig. 6) and assuming 0.7 Mtpa average injection rates, we can infer that:

- A single 'Gulf-of-Mexico well development' CO_2 injection model could achieve the 7 Gtpa storage by 2043 and 12 Gtpa by 2050. Cumulative storage in 2050 would be 116 Gt.
- Alternatively, five 'Norway offshore well development' models could achieve the 7 Gtpa storage by 2050. Cumulative storage in 2050 would be 73 Gt.
- Cumulative storage of >100 Gt by 2050 is most efficiently achieved with 5-7 regions pursuing a Norwegian-scale offshore well development model using individual well injection rates between 0.5-1 Mta, although it could be achieved with a single GoM model with 0.7 Mtpa injection rates.

The point of this extrapolation is to demonstrate that it will only take a fraction of the historic worldwide offshore petroleum well development rate to achieve the global requirements for GCS. While offshore CCS is suitable many places (recall Figs 1 and 2), it does not have to be deployed everywhere to achieve global benefit, and focus can be on the most prospective and economic regions. In practice, these developments would likely occur in multiple offshore basins close to the main locations of onshore capture; however, our selected basin development curves constrain the total well rate required to achieve the incremental and cumulative 2DS emissions reduction goal for 2050. Further discussion of the assumptions made in this evaluation and alternative injection wells scenarios are given in the methods paper[9].

To obtain a preliminary cost estimate for this potential global offshore drilling programme, we note that offshore injection well costs are of order ~50-100M€ (55-110 MUSD) per well, assuming a 2015 reference case[55]. The offshore drilling costs in terms of emissions avoided are therefore of order 2.9-5.5 €/tonne (3.2-6.3US$/tonne) for our mean well rate of 17.5Mt per well. This does not include the costs of capture, transport or platform infrastructure, but indicates that offshore saline aquifer storage can be a cost-effective emissions-mitigation measure in a world where the cost of emitting to atmosphere rises above the current level of 20-60 US$/tCO2e (carbonpricingdashboard. worldbank.org).

Conclusions

CCS is essential for realizing a global emissions reduction strategy consistent with 2DS aspirations. Globally, it is the continental margin geology that can most rapidly accommodate the large-scale CCS anticipated. There are many well-established global geologic similarities in these basins, and prior petroleum exploration provides an exceptionally well-documented starting point for deploying CCS in these settings. We propose using the characteristic pressure and stress versus depth trends in these basins as a framework for determining the initial and final pressure bounds (the basin ΔP approach) for determining the capacity of prospective storage projects. By utilizing the 'pressure stratigraphy' of these basins, early class-A projects can exploit the most accessible storage sites (generally shallower and less constrained by pressure limits), while later projects will exploit the majority of sites (class-B projects) which will have practical pressure limits governed by the basin stress and pressure profiles. Eventually, more advanced technology using pressure management approaches (class-C projects) will allow further resource development. This forward strategy for CCS has a precedent in the historic development of technology in oil and gas projects.

The timeframe of Gigatonne-scale CCS is hard to evaluate using either multiple individual numerical reservoir simulations (too many are needed) or using regional static volumetric assessments (which are likely optimistic as they don't account for the dynamic pressure conditions). However, by developing a basin-scale pressure model to frame project capacity assessments, we propose a consistent and transparent basis for assessing and developing these resources.

Using historic well development scenarios from mature hydrocarbon basins and applying stratigraphic dynamic pressure constraints, a strategy for accessing the required storage capacity through time is demonstrated, providing a roadmap for global deployment of offshore CO_2 storage consistent with the 2DS objective. Using this analysis, it is clear that the required well rate for realizing

global CCS in the 2020-2050 timeframe is a manageable fraction of the historical well rate deployed from historic petroleum exploitation activities and is most efficiently achieved with multiple simultaneous regional developments.

Author contributions statement:

P.R. mainly contributed the work on CO_2 injectivity, well rates, basin pressure analysis and the offshore Norway case study. T.M. mainly contributed the work on global offshore basins and hydrocarbon fields and the Gulf of Mexico case study. Well databases were assessed by T.M. and the injection-well model scenarios were mainly developed by P.R. Both authors worked iteratively to develop the arguments.

Competing Interests statement:

The authors do not consider there to be any competing interests related to this submission.

Data availability statement:

Methods used are described in the supporting methods paper (or Appendix).

Acknowledgements

P. R. thanks NTNU and Equinor for financial support and permission to publish and acknowledges useful advice from Bamshad Nazarian (Equinor), Ole Jakob Artnzen (Equinor) and Martin Landrø (NTNU). CO_2 storage site data from Equinor operations was kindly released to NTNU as part of the Norwegian CCS Research Centre. T.M. thanks his colleagues at the Gulf Coast Carbon Center for constructive discussions, the Director of the Bureau of Economic Geology, The University of Texas at Austin for authorization to publish, and research funding in part through National Energy Technology Laboratory DOE award number: DE-FE0026083 - Offshore CO_2 Storage Resource Assessment of the Northern Gulf of Mexico. The views and opinions of authors expressed herein do not necessarily state or reflect those of our host institutions, or the United States Government or any agency thereof.

References

1. Stocker, T. F. (Ed.) Climate change 2013 - the physical science basis. Working Group I contribution to the Fifth assessment report of the Intergovernmental Panel on Climate Change (Cambridge University Press, 2014).
2. IEA, 20 years of carbon capture and storage: Accelerating future deployment. https://www.iea.org/publications (2016).
3. IEA, Energy Technology Perspectives in 2017 (OECD/IEA. Paris, 2017)
4. Pacala, S. & Socolow, R. Stabilization Wedges: Solving the Climate Problem for the Next 50 Years with Current Technologies, *Science*: 305 (5686): 968-972 DOI: 10.1126/science.1100103 (2004).
5. IEA, Carbon Capture and Storage: The solution for deep emissions reductions (International Energy Agency Publications, Paris, 2015)
6. Edenhofer, O. et al., (Eds), Mitigation of Climate Change. Working Group III (WG3) of the Fifth Assessment Report (AR5) of the Intergovernmental Panel on Climate Change. (Cambridge University Press, 2014).
7. Alcalde, J., Flude, S., Wilkinson, M., Johnson, G., Edlmann, K., Bond, C. E., ... & Haszeldine, S. R., Estimating geological CO_2 storage security to deliver on climate mitigation, *Nature Communications*, *9*, [2201]. DOI: 10.1038/s41467-018-04423-1. (2018)
8. GCCSI, Global status of CCS: 2018, www.globalccsinstitute.com/resources/global-status-report/ (Global CCS Institute, 2018)
9. See Appendix: Methods used in supporting the main paper
10. Van der Meer, L.G.H., The CO_2 storage efficiency of aquifers, *Energy Conversion and Management,* 36(6-9): 513-518. (1995)
11. IEAGHG, CCS Deployment in the context of regional developments in meeting long-term climate change objectives (IEAGHG Technical Report 2017-07, August, 2017).
12. Divins, D.L., Total Sediment Thickness of the World's Oceans & Marginal Seas, NOAA National Geophysical Data Center, Boulder, CO. (2003).
13. Whittaker, J. et al., Global sediment thickness data set updated for the Australian-Antarctic Southern Ocean, Geochemistry, Geophysics, Geosystems, 14(8): 3297-3305 (2013).
14. Mann, P., Gahagan, L., and Gordon, M., Tectonic Setting of the World's Giant Oil Fields, *World Oil* 222.10 (October): 78–79 (2001).
15. Schlee, J.S., A comparison of two Atlantic-type continental margins, U.S. Geological Survey, Professional Paper 1167 (United States Government Printing Office, Washington D.C., 1980)
16. Gibbs, A.D., Structural evolution of extensional basin margins, *J. Geol. Soc. London*, 141: 609-620 (1984)

17. Lister, G.S., Etheridge, M.A. & Symonds, P.A. Detachment models for the formation of passive continental margins, *Tectonics,* 10(5): 1038-1064 (1991).
18. Ehrenberg, S.N., and Nadeau, P.H. Sandstone vs. carbonate reservoirs: a global perspective on porosity-depth and porosity-permeability relationships, *AAPG Bulletin,* 89(4): 435-445 (2005).
19. Smith, D. A., Sealing and non-sealing faults in Louisiana Gulf Coast Basins: *AAPG Bulletin,* 64, 145–172 (1980).
20. Manzocchi, T., Childs, C., and Walsh, J. J., Faults and fault properties in hydrocarbon flow models. *Geofluids,* 10(1-2), 94-113 (2010).
21. U.S. Geological Survey, World Petroleum Assessment 2000, Digital Data Series 60, https://energy.usgs.gov/OilGas/AssessmentsData/WorldPetroleumAssessment.aspx (2000).
22. Huffman, A.R. & Bowers, G.L. Pressure regimes in sedimentary basins and their prediction, *AAPG Memoir 76*, https://doi.org/10.1306/M76870. (2001)
23. Harrison, W. J., and Summa, L. L. ,1991, Paleohydrology of the Gulf of Mexico basin. American Journal of Science, 291(2), 109-176.
24. Gaarenstroom, L., Tromp, R. A. J., & Brandenburg, A. M., 1993, Overpressures in the Central North Sea: implications for trap integrity and drilling safety. In Geological Society, London, Petroleum Geology Conference series, Vol. 4, No. 1: 1305-1313.
25. Mello, U. T., and Karner, G. D., 1996, Development of sediment overpressure and its effect on thermal maturation: Application to the Gulf of Mexico basin. AAPG bulletin, 80(9), 1367-1396.
26. Bolås, H. M. N., and Hermanrud, C., 2003, Hydrocarbon leakage processes and trap retention capacities offshore Norway, Petroleum Geoscience, 9(4): 321-332.
27. Ramdhan, A. M., & Goulty, N. R. Overpressure and mudrock compaction in the Lower Kutai Basin, Indonesia: A radical reappraisal. *AAPG bulletin*, 95(10), 1725-1744 (2011).
28. Muggeridge, A., Y. Abacioglu, W. England, and C. Smalley, The rate of pressure dissipation from abnormally pressured compartments, *AAPG Bulletin,* 89(1): 61-80 (2005).
29. Osborne, M. J., and Swarbrick, R. E. Mechanisms for generating overpressure in sedimentary basins: A reevaluation. *AAPG bulletin,* 81(6), 1023-1041 (1997).
30. Seni, S.J. et al. (Eds.) Atlas of Northern Gulf of Mexico Gas and Oil Reservoirs, Volume 1 - Miocene and Older Reservoirs. (Bureau of Economic Geology, The University of Texas at Austin, 1997).
31. Meckel, T.A., Nicholson A.J. & Treviño, R.H. Capillary aspects of fault-seal capacity for CO_2 storage, Lower Miocene, Texas Gulf of Mexico, In: Treviño, R.H., and T.A. Meckel, Eds., Geological CO_2 sequestration atlas of Miocene strata, offshore Texas state waters, Bureau of Economic Geology, Report of Investigations No. 283 (The University of Texas at Austin, 2018).
32. Morris, S., B. Vestal, K. O'Neill, M. Moretti, C. Franco, N. Hitchings, J. Zhang, & J.D. Grace, The pore pressure regime of the northern Gulf of Mexico: Geostatistical estimation and regional controls, *AAPG Bulletin*, 99(1): 91-118 (2015).
33. Birkholzer, J.T., Zhou, Q., Cortis, A., Finsterle, S. A sensitivity study on regional pressure buildup from large-scale CO2 storage projects. *Energy Procedia*, 4, 4371–4378. http://dx.doi.org/10.1016/j.egypro.2011.02.389. (2011).
34. Ganjdanesh, R. & Hosseini, S.A. Development of an analytical simulation tool for storage capacity estimation of saline aquifers, *Int. J. Greenhouse Gas Control,* 74: 142-154 (2018).
35. Rutqvist, J., Birkholzer, J.T., Tsang, C.-F. Coupled reservoir-geomechanical analysis of the potential for tensile and shear failure associated with CO_2 injection in multilayered reservoir–caprock systems. *International Journal of Rock Mechanics and Mining Sciences*, *45*(2), 132-143. http://dx.doi.org/10.1016/j.ijrmms.2007.04.006. (2008).
36. Mathias, S.A., Miguel de, G.J.G.M., Thatcher, K.E., Zimmerman, R.W. Pressure buildup during CO2 injection into a closed brine aquifer. *Transport Porous Media* 89, 383–397. http://dx.doi.org/10.1007/s11242-011-9776-z. (2011).
37. Ehlig-Economides, M. J. and Economides, C. A., Sequestering Carbon Dioxide in a Closed Underground Volume. *Journal of Petroleum Science and Engineering*, 70, 123-130 (2009).
38. Cavanagh, A.J., Haszeldine R. S. and Blunt M. Open or Closed: A Discussion of the Mistaken Assumptions in the Economides Analysis of Carbon Sequestration. *Journal of Petroleum Science and Engineering,* 74(1-2), 107-110 (2010).
39. Babaei, M., R. Govindan, A. Korre, J-Q. Shi, S. Durucan, M. Quinn, Calculation of pressure- and migration-constrained dynamic CO_2 storage capacity of the North Sea Forties and Nelson dome structures, *International Journal of Greenhouse Gas Control,* 53:127-140 (2016).
40. Goudarzi, A., S.A. Hosseini, D. Sava, and J-P Nicot, Simulation and 4D seismic studies of pressure management and CO_2 plume control by means of brine extraction and monitoring at the Devine Test Site, South Texas, USA, *Greenhouse Gas Sci. Technol.* 8:185-204 (2017).
41. Metz, B., Davidson, O., De Coninck, H., Loos, M. and Meyer, L. *Carbon dioxide capture and storage:* Working Group III of the Intergovernmental Panel on Climate Change (Cambridge, University Press, United Kingdom and New York, USA (2005).
42. Birkholzer, J. T., Zhou, Q., & Tsang, C. F. Large-scale impact of CO_2 storage in deep saline aquifers: A sensitivity study on pressure response in stratified systems, *International Journal of Greenhouse Gas Control,* 3(2): 181-194 (2009).
43. Hansen, O., Gilding, D., Nazarian, B., Osdal, B., Ringrose, P., Kristoffersen, J. B., ... & Hansen, H. Snøhvit: The history of injecting and storing 1 Mt CO_2 in the fluvial Tubåen Fm. *Energy Procedia*, 37, 3565-3573 (2013).
44. Pawar, R. J., Bromhal, G. S., Carey, J. W., Foxall, W., Korre, A., Ringrose, P. S., ... & White, J. A. Recent advances in risk assessment and risk management of geologic CO2 storage. *International Journal of Greenhouse Gas Control,* 40, 292-311 (2015).

45. Gasda, S. E., Nordbotten, J. M., & Celia, M. A. Vertically averaged approaches for CO_2 migration with solubility trapping. Water Resources Research, 47.5 (2011)
46. Gasda, S. E., Nilsen, H. M., & Dahle, H. K. Impact of structural heterogeneity on upscaled models for large-scale CO2 migration and trapping in saline aquifers. *Advances in Water Resources*, 62: 520-532 (2013).
47. Buscheck, T. A., Sun, Y., Chen, M., Hao, Y., Wolery, T. J., Bourcier, W. L., ... and Aines, R. D. Active CO_2 reservoir management for carbon storage: Analysis of operational strategies to relieve pressure buildup and improve injectivity, *International Journal of Greenhouse Gas Control,* 6, 230-245 (2012).
48. Nazarian, B., Thorsen, R & Ringrose, P. Storing CO_2 in a reservoir under continuous pressure depletion – a simulation study, GHGT-14 Conference Proceedings, Melbourne, Australia. (In press, 2019)
49. Jenkins, C. R., Cook, P. J., Ennis-King, J., Undershultz, J., Boreham, C., Dance, T., ... and Kirste, D. Safe storage and effective monitoring of CO2 in depleted gas fields. *Proceedings of the National Academy of Sciences,* 109(2), E35-E41 (2012).
50. Thibeau, S., Seldon, L., Masseranoc, F., Canal Vila, J. and Ringrose, P. Revisiting the Utsira Saline Aquifer CO2 Storage Resources using the SRMS Classification Framework. GHGT-14 Conference Proceedings, Melbourne, Australia. (In press, 2019)
51. Bøe R., Magnus C., Osmundsen P.T., Rindstad B.I. CO_2 point sources and subsurface storage capacities for CO_2 in aquifers in Norway, Norwegian Geological Survey (NGU) Report 2002.010 (2002).
52. Gasda, S., Wangen, M., Bjørnara, T., Elenius, M. Investigation of caprock integrity due to pressure build-up during high-volume injection into the Utsira formation. *Energy Procedia,* 114, 3157-3166. (2017)
53. Holloway S. (Ed.) The underground disposal of carbon dioxide, Final report of Joule 2, Project No. CT92-0031, British Geological Survey, Keyworth, Nottingham, UK, 355p. (1996).
54. International Energy Agency Energy: Technology Perspectives 2013: Technology Roadmap for Carbon Capture and Storage (p.23-24; 2013).
55. Ringrose, P., Furre, A. K., Bakke, R., Dehghan Niri, R., Paasch, B., Mispel, J., ... & Hermansen, A. Developing Optimised and Cost-Effective Solutions for Monitoring CO_2 Injection from Subsea Wells. In 14th Greenhouse Gas Control Technologies Conference Melbourne (2018).

Appendix: Methods used in supporting the main paper

A1 Offshore Basins – methods and uncertainties

It is very challenging to summarize the cumulative efforts over several decades in characterization and understanding the geologic development of offshore sedimentary basins. Broad patterns are predictable, while specific elements may differ depending on basin history. However, to reinforce our generalizations we briefly synthesize prior work and illustrate the character of six selected basins based on published studies (Figure A1). One of the main achievements of stratigraphic studies since the 1970's has been the development of sequence stratigraphic concepts that allowed interpretation of passive continental margin stratigraphy in the context of global relative sea level variation[1], and the subsequent application of those predictive concepts in subsurface seismic stratigraphic interpretation[2,3] allowing broad stratigraphic comparisons to be made among different basins. The effectiveness of this understanding was exemplified by rapid methodical expansion of global hydrocarbon exploration. Such exploration efforts have provided an advanced understanding of subsurface fluid pressure distributions, and the geologic conditions favorable for retaining hydrocarbon accumulations[4,5,6]. Observed similarities between basins led to concepts for classifying the basin hydrodynamic and petroleum systems, providing important concepts that also apply to GCS, such as rates of vertical and lateral drainage, the development and dissipation of overpressure[7] and the nature of petroleum migration and retention[8,9]. Over a similar timeframe, the global subsurface stress distribution has been cataloged globally using extensive well data[10]. These are not new findings, which is exactly the point: GCS can evolve from a very mature understanding of geologic, tectonic, and fluid history. This advanced level of integration of stratigraphy, fluid pressure, and stress fields provides an exceptional technical basis for pursuing gigatonne-scale CCS. These continental margin settings have retained tremendous volumes of hydrocarbon resources (Fig. 1; Ref [11]), providing a strong indication of highly suitable subsurface geologic conditions for Gt-scale CO_2 disposal.

There are certainly important basinal differences: some basins have significant salt tectonic components (Brazil, Gulf of Mexico), others are seismically active (Pacific USA, southeast Asia), and yet others at high latitudes have significant geologically-recent vertical tectonic components due to Quaternary glacial cycles (e.g. the North Sea[12,13]). The timing of the main rifting phase may also vary significantly, such as offshore NW Australia[14]. Additionally, not all continental margins are passive, with those on the Pacific Rim being more tectonically active (compressional, translational). Furthermore, not all Cenozoic extensional settings have experienced the same extensional rates, durations, and magnitudes, which contribute to significant basinal differences, mostly in structural style but also in stratigraphic thickness (isopach). The provenance (source geology) of clastic sediments can create notable sediment compositional differences (most significantly feldspar and volcanic fragment content) that could be significant for long-term subsurface CO_2 mineralization during CCS. Despite these differences, at a first order there appears to be globally-equitable distribution of high-quality potential storage resources on continental margins (Figs. 1 and 2; Ref [11]).

Table A1 and Figure A2 show example functions we have used to describe stress and pressure profiles in two example basins – the Norwegian North Sea (NNS) and the Gulf of Mexico (GoM).

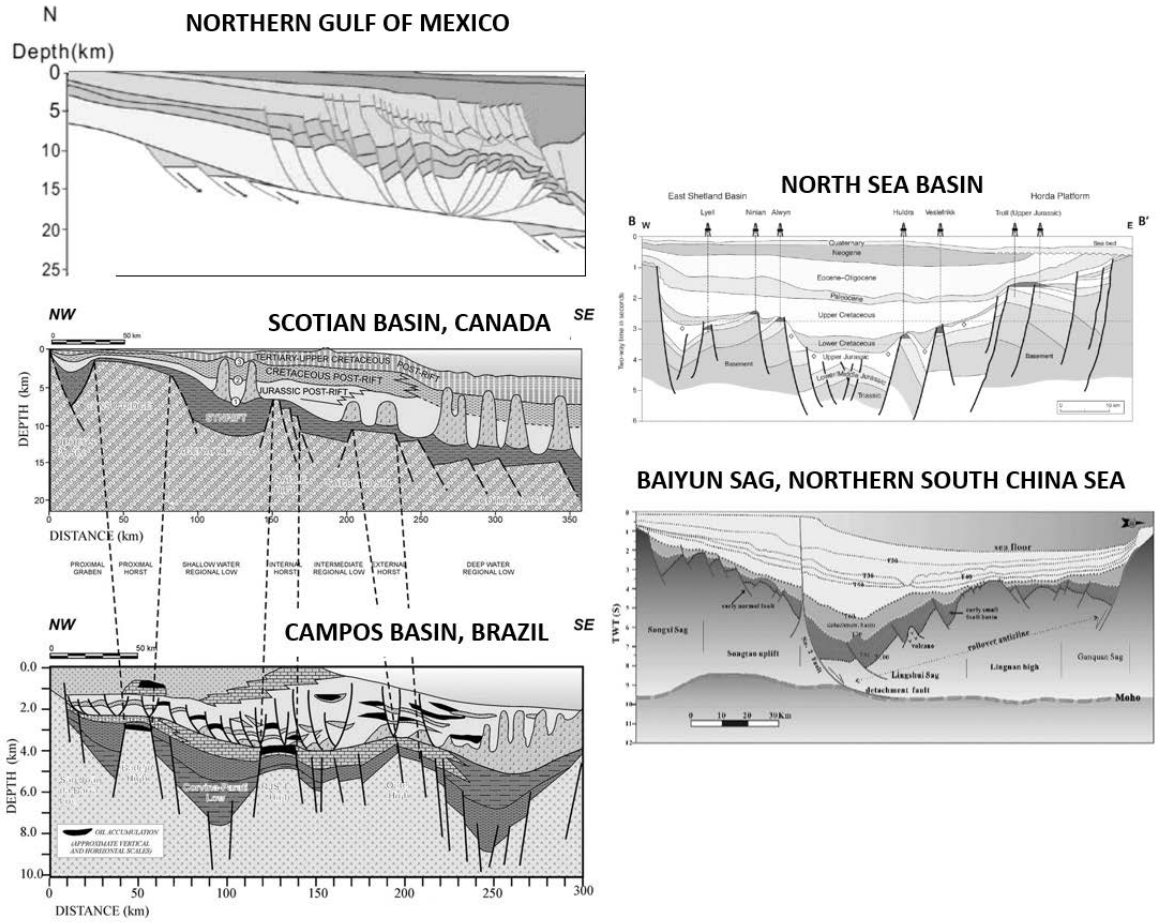

Figure A1. Comparison of previously interpreted schematic geologic cross sections from various passive extensional continental margins, showing broad stratigraphic and structural similarities: deep Mesozoic extensional faults, overlain by a progradational Late Mesozoic to Cenozoic section [Figure sources: Northern Gulf of Mexico[15](https://creativecommons.org/licenses/by-sa/3.0/), North Sea[6] (This figure is not covered by the CC BY license, © Geological Society of London, All rights reserved, used with permission), Scotian Basin[16] (this figure is not covered by the CC BY license, © Geological Society of London, All rights reserved, used with permission), Campos Basin[16] (this figure is not covered by the CC BY license, © Geological Society of London, All rights reserved, used with permission) and Baiyun Sag[17]].

Parameter	Norwegian North Sea case	Comments/Sources	Gulf of Mexico case	Comments/Sources
Seabed temperature	Assumed constant at 5°C	Ref[18]	15-25°C seasonally for inner-shelf water depths < 60 m	Ref[19]
Geothermal gradient	35°C/km	Ref[20]	23°C/km to 3,000 m increasing below to 34°C/km	Ref[21] Figure 4.5; Ref[22]
Brine density	1020 kg/m^3 to 1 km depth; increasing by 60 kg/km from 1 km downwards	Close to sea water density in shallow section; matches observations at Sleipner[20] and Snøhvit	Average (N=66) of 1070 kg/m^3 for Texas Miocene interval (1-3 km)	Supplementary Material[23]; produced waters database[24]
Poisson's ratio	0.1 at surface increasing by 0.06/km with depth toward 0.4 at 5km	General match to well data used to estimate fracture pressure[6]	0.2 near surface increasing to 0.5 at 6 km depth	Ref[25]; Ref[26] (Eqn. 7)
Bulk rock density	2000 kg/m^3 at surface; 2750 at 5km; constant gradient of 150 kg/km	General match to well data used to estimate vertical stress functions[6]	2000 kg/m^3 near surface, reaching 2450 at 5 km depth.	Ref[25]

Table A1. Functions used to describe stress and pressure profiles in two example basins – NNS and GoM.

A2 Offshore storage resources – methods and uncertainties

CO_2 storage resources have been quantified in a number of national CO_2 storage atlases[28,29,30,31] and other studies[32,33,34] which support the general conclusion that there are thousands of Gt of potential offshore storage space (static pore volumes) that are favorable for near-term CCS maturation in any given global offshore region. For example, the US NETL Atlas[31] has offshore Saline Aquifer Formation (SAF) static storage capacity between 472 and 6433 billion metric tons, with a medium estimate of 2277 billion metric tons (Gt). These regional static volumetric assessments have necessarily used relatively simplified methods, and recent research indicates that capacity estimates that incorporate pressure limitations may be a factor of ten lower than estimates based on pore volume[35]. Furthermore, availability of potential resources for storage may also conflict with other users (including oilfield developments, wind-farm leases, and protected marine habitats), and areas with water depths greater than 1,000 meters (Ref[11] Fig. 2) may slow development pace, leading to some practical restrictions. However, even with these limiting factors the continental margin basins have several hundreds of Gt of storage available for development in the 2020-2050 timeframe. Figure A3 shows an example of the storage resource for the Norwegian North Sea basin where 45.4 Gt of storage resources have been mapped[30], with 16.8 Gt in the Cenozoic sequences and a further 28.6 Gt in the Mesozoic units. Equivalent capacity estimates for the Gulf of Mexico Cenozoic stratigraphy are around 558 Gt (Figure A4).

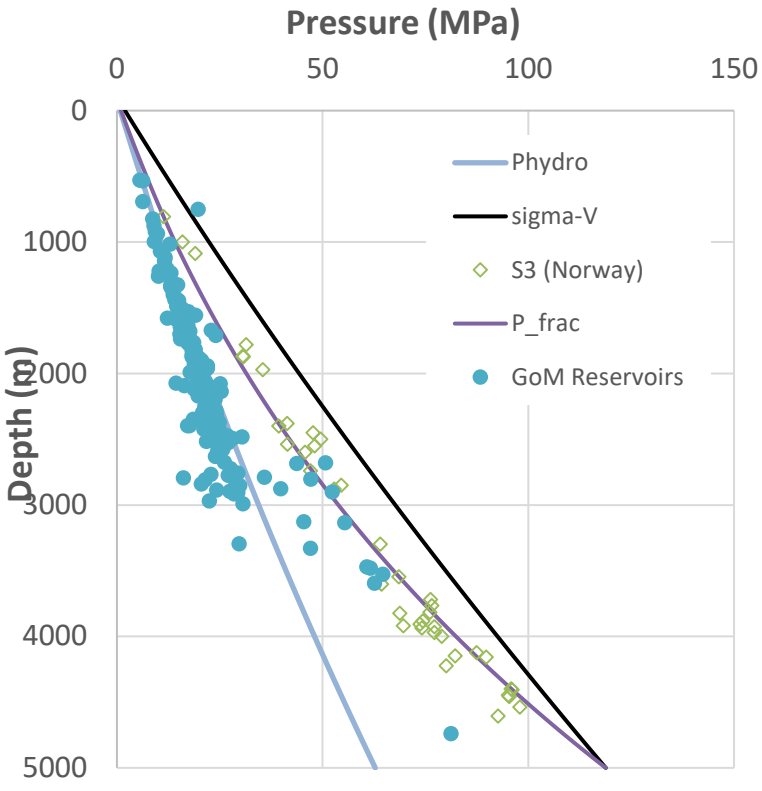

Figure A2. Basin depth functions for Norwegian North Sea with minimum stress data (S3) from Ref[6] compared with GoM reservoir fluid pressures for Miocene age reservoirs in the Texas portion of the Gulf of Mexico[27]

Where national authorities have mapped the available resources for geological storage of CO_2 in saline aquifers, these resource assessments generally estimate the available pore volume in porous geological rock units, scaled by a storage efficiency factor, ε, where ε is the fraction of the available pore space occupied by CO_2. This storage efficiency factor attempts to capture the physical process of CO_2 drainage into a water-wet brine-filled rock formation. Estimates for ε are typically around 4%,

although local factors may render values between 1% and 6% with lower values generally corresponding to pressure-limited storage units. These estimates are founded on the principles of fluid dynamics whereby a buoyant non-wetting fluid displaces the in situ wetting fluid (brine) in a process controlled by the fluid mobility ratio and the gravity number[36,37]. We do not dispute the utility of using these storage efficiency factors to describe and quantify potential subsurface storage capacity but rather consider them to be insufficient for informing practical deployment of that global resource. Indeed, the long-running Sleipner project which demonstrates a storage efficiency of 5% after 22 years of injection provides some validation that these estimates for ε are operationally reasonable[38].

Figure A5 shows an example of storage resource mapping from the Norwegian North Sea basin[30], where we have added error bars based on the likely ranges for ε. When including these uncertainty ranges, there is still clearly a substantial resource available, with the total basin storage resource estimate lying between 10.5 Gt and 56 Gt (median = 45.4 Gt). The problem is not the availability of the storage resources, but rather the practical, temporal and economic means of exploiting the resource. A similar analysis for the GoM dataset (Figure A4) gives a range of 140 to 698 Gt around the median value of 558 Gt.

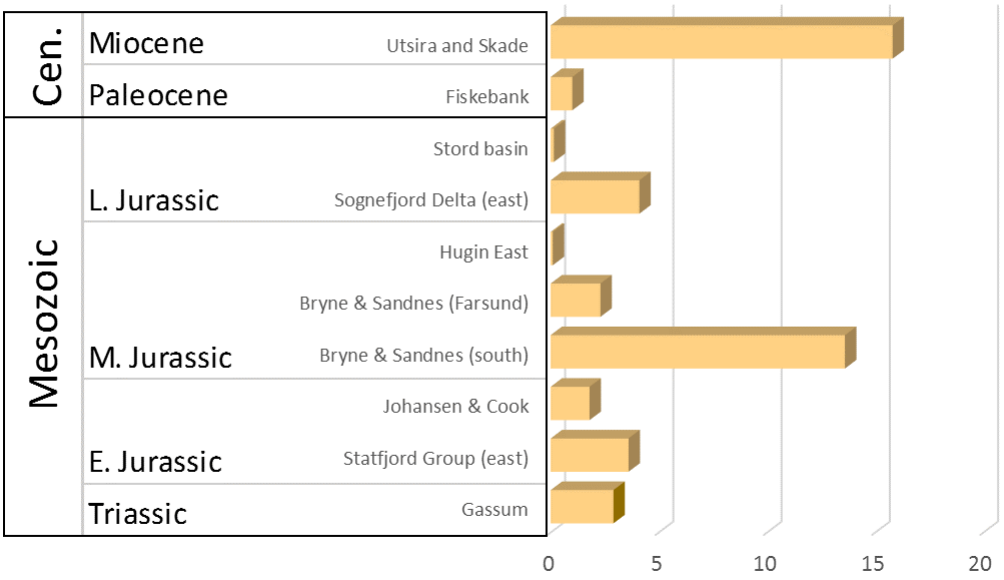

Figure A3. Stratigraphic disposition of CO_2 storage resources for the Norwegian North Sea basin with capacity estimates from Ref[30]

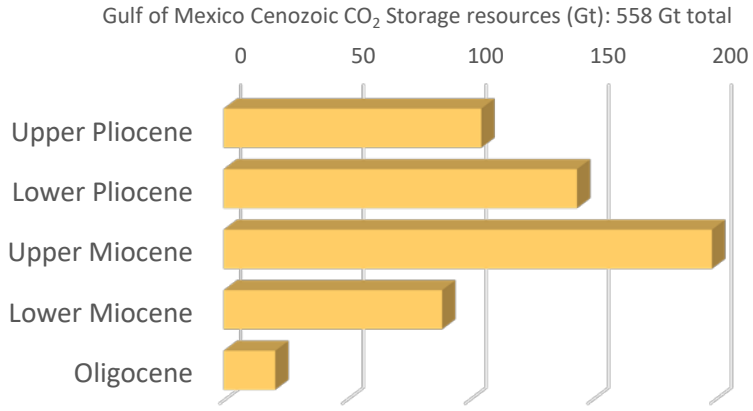

Figure A4. Stratigraphic disposition of CO_2 storage resources for the Cenozoic portion of Gulf of Mexico inner shelf basin with capacity estimates from Gulf Coast Carbon Center.

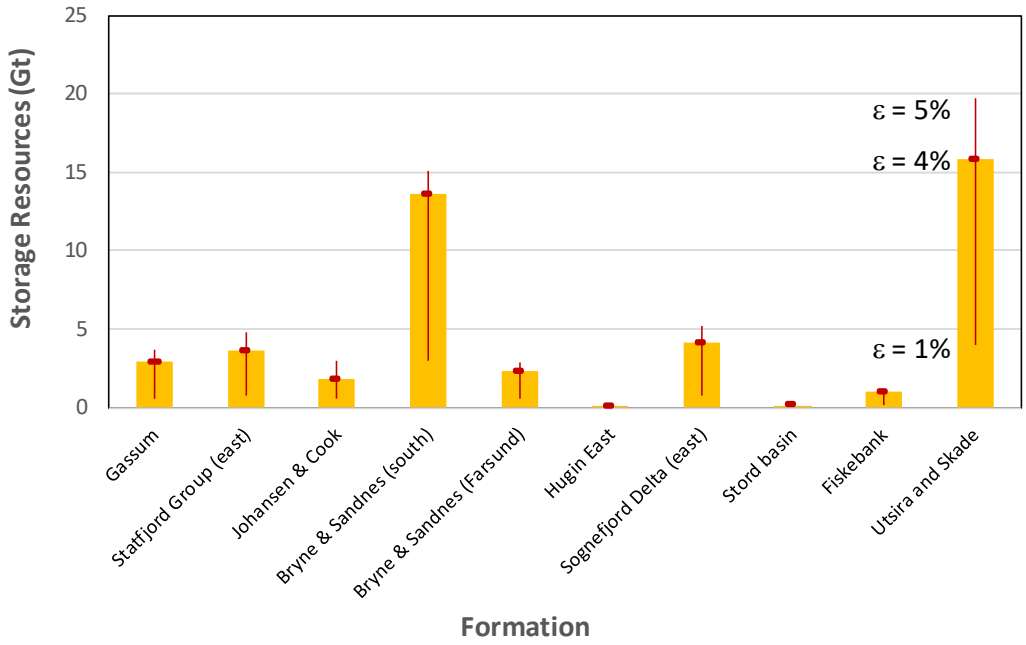

Figure A5. Example of mapped CO_2 storage resources for the Norwegian North Sea basin[30], with error bars based on the storage efficiency factor, ε. Actual values for ε are shown for the Utsira and Skade Formation case.

A3 Derivation of functions for the basin fluid pressure analysis approach

We have addressed the problem of offshore storage resource assessment by using a generic approach based on pressure and stress trends in offshore sedimentary basins. For the case of non-infinite saline aquifers bounded by some set of structural or stratigraphic barriers, pressure will generally add a limiting factor to storage capacity estimates based on fluid dynamics of open systems. For any subsurface injection project, the geomechanical strength of the confined or semi-confined aquifer gives a practical limit to maximum allowable injection pressure, P_{max}, which is defined with reference to the fracture pressure, P_{frac}, of the relevant confining rock units. The definition of P_{frac} is complex and depends on the stress field, the borehole orientation and the *in-situ* rock properties[25,39,40]. The value for P_{frac} is generally close to (but not equal to) the minimum in situ stress component, σ_3, of the stress tensor. For the purposes of this discussion we use an upper-bound estimate of the fracture pressure[40,41], appropriate for vertical wells in sedimentary basins:

$$P_{frac} = \frac{2\nu}{1-\nu}(\sigma_V - P) + P \qquad (1)$$

where ν is Poisons ratio, σ_V is the vertical (overburden) stress and P is the pore pressure.

For any specific CO_2 storage project, we can then define the available pressure range for injection:

$$\Delta P = P_{max} - P_{init} \approx P_{frac} - P_{init} \qquad (2)$$

To define the initial pressure condition, we need to have some knowledge of the basin history. For this analysis we consider two well-known basins – the North Sea (Norway) and the Gulf Coast (USA) – where we have a good knowledge base from several decades of oil and gas exploration and production. Figure A2 (and Fig. 3 main paper[11]) shows the general situation in the Norwegian North Sea and Gulf of Mexico. Most saline aquifer formations are normally pressured (i.e. close to the

hydrostatic pressure, P_{hydro}) in the upper 2-3 km interval. In these intervals $P_{init} \approx P_{hydro}$. The deeper units which tend to be over-pressured, will then have $P_{init} > P_{hydro}$. A further important factor for definition of P_{init} is that pressure depletion in oil and gas fields may cause depleted initial pressures in saline aquifer formations which are hydraulically connected to the hydrocarbon resource. These production-related pressure depletions may negate initial overpressures or even take initial pressures below P_{hydro}. We will address the interactions between emerging developments of saline storage resources and hydrocarbon resource developments in the subsequent discussion.

The performance of a CO_2 injection well can be summarized by the Injectivity Index, II_{CO2}, which for the simplest case is given by:

$$II_{CO2} = \frac{q}{(p_{fbhp} - p_{res})} \quad (3)$$

where q is the well flow rate and p_{fbhp} is the flowing bottom-hole pressure and p_{res} is the far-field reservoir pressure. In practice, several other terms may need to be included in the function to account for near-wellbore effects and pressure and temperature gradients within the wellbore[42,43]. Injectivity may also vary as a function of time due to, for example, near-wellbore geochemical and geomechanical processes and long-term trends in far-field reservoir pressure[44].

To generalize the long-term performance of an injection well in a saline aquifer we adapt the equation for radial flow around a wellbore[42] to give an integrated function for the flow rate over the lifetime of the injection well in the time interval *i* to *f*:

$$\int_i^f q_t = \frac{2\pi k_a h_a}{\mu \ln\left(\frac{r_e}{r_w}\right)} \left[\int_i^f (p_{well} - p_{res}) \right] \quad (4)$$

where k_a is the permeability of the aquifer formation, h_a is the height of the injection well interval, μ is the CO_2 viscosity, r_e is the effective radius of the reservoir unit and r_w is the radius of the well. Generalizing this function and adding a flux term, F_b, to represent a flux boundary condition for the injection unit, we have:

$$V_{injected} = I_C \int_i^f (p_{well} - p_{res}) - F_b \quad (5)$$

where $V_{injected}$ is the total volume injected over the project lifetime and I_c is a constant equivalent to the mean Injectivity index. For a closed saline aquifer unit with no-flow boundary conditions (such as a sealed fault block), $F_b = 0$. If there is some pressure dissipation from the saline aquifer formation, F_b is positive, while a case with some brine influx into the storage unit has negative F_b. It is assumed that F_b is normally a small factor compared to the injectivity term. However, for the case of an infinite aquifer with no pressure boundary limitation, F_b could be large or even dominant. The integral of reservoir pressure with time will be a function of the formation properties and the dimensions of the storage unit (main paper[11] Fig. 4). This pressure function would normally be estimated using reservoir simulation of numerical models of the complex basin architecture (including effects faults and internal rock heterogeneity). However, general experience and knowledge of pressure propagation in porous media, suggests that the pressure will follow a characteristic function of time, based on pressure transient analysis[45,46], where the dimensionless pressure function has the form:

$$p_D(t_D) = \frac{1}{2} \ln\left(\frac{4t_D}{\gamma}\right) \quad (6)$$

where p_D is dimensionless pressure, t_D is dimensionless time and γ is 1.781 (related to Euler's constant). The coefficient of ½ may lie above or below this value depending on the reservoir boundary conditions (open, closed, or transient), but is assumed to be ½ for this analysis. Effects of compressibility of CO_2 are omitted in this analysis, being a short-term transient effect, while the

compressibility of the total fluid-rock system is embedded in the p_D function. To apply this equation in real dimensions for a pressure build-up case we can define:

$$p_{res}(t) = p_{init} + A\, p_D(t_D) \qquad (7)$$

where A is a scaling parameter (related to the reservoir characteristics). Combining equations 5 and 7, we can obtain a general equation for the storage volume as a function the pressure bounds:

$$V_{project} = I_C \left[p_{well} - p_{init} + \int_i^f A\, p_D(t_D)\right] + F_b \qquad (8)$$

It should be emphasized that Equation 8 assumes a constant injection pressure and constant injectivity – simplifying assumptions appropriate for screening prospective projects. With more complex operational variables, numerical reservoir simulation can be used to more accurately assess injection volumes as a function of variable pressure gradients. At the project screening stage, parameters for Equation 8 can be estimated using regional basin data and initial estimates of storage unit geometry and formation permeability. Volumes are converted to mass using estimates for the mean in situ density. For more detailed project designs, high-resolution digitized reservoir simulation models would be needed.

To illustrate the utility of the pressure-based method for estimation of CO_2 storage volumes, we apply Equations 6-8 to the known pressure history at the Snøhvit CO_2 injection project offshore Norway. Here we consider only a 3-year injection period for the Tubåen reservoir, which was followed by a second injection phase into a different shallower reservoir unit[47]. Here the bottom-hole pressure (BHP) is measured at a gauge 800m above the reservoir[47] allowing BHP to be estimated accurately. We first re-scaled the dimensionless pressure function to the observed pressure history, assuming p_{init} = 290 bars and A = 34 (with time measured in months), to give the function P_{res} (Fig. A6) using Equation 7. Assuming a constant P_{well} of 380 bars, we then calculate the volume injected assuming I_c = 40 m^3/day/bar (the expected injectivity prior to project start-up[48]), using Equation 8. The result is 1.13 Mt injected over the 34-month period (June 2008 to April 2011). This is slightly higher than the actual injected volume of 1.09 Mt, a reasonable error given that actual injection history was affected by stoppages. Also, we assume F_b is negligible for this example.

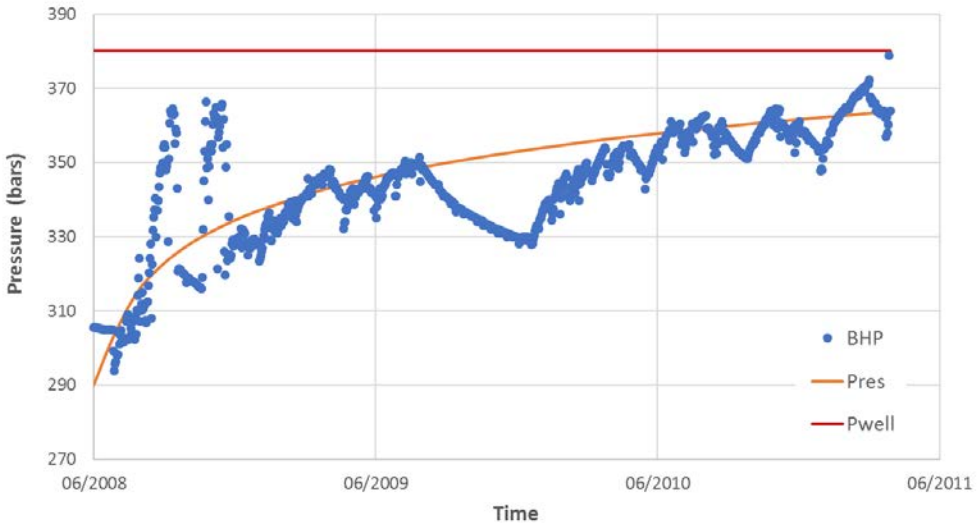

Figure A6. Pressure functions used to make a simplified storage volume estimate for the Snøhvit injection case.

A4 Historic CO_2 injection well data

Summary statistics for published industrial-scale SAF injector wells (used as basis for future injection-rate scenarios) are shown in Tables A2 and A3, with the statistical distributions of the data alongside the model scenarios used in the paper shown in Figure A7. The dataset comprises 60 years of injection data from 9 wells, with a mean rate of 0.532±0.271 Mt/year. For the offshore wells the mean rate is 0.695±0.222. We infer that 0.7Mt/year/well is a realistic average rate for the offshore case. The P90-P10 range is 0.330-1.059, which has been used to define confidence intervals the future well scenarios (P90 refers to 90% probability of exceedance). Higher injection rates are technically possible (of order 2 Mtpa per well) and future technology development is expected to lead to a future mean rate of closer to 1.0 Mt/year/well. Figure A8 shows the pressure functions for the four model scenarios (Main paper[11]) chosen to represent the range of expected behavior.

Project	Sample (injection years)	Injection rate per well (Mt/year)	Equiv. rate (t/hour)	Estimated formation permeability (Darcy) / porosity
Sleipner (peak)	1	1.01	115	1-8 / 0.36
Sleipner (mean) [16, 34]	21	0.85	97	
Snøhvit-Stø (mean)	8	0.61	70	0.01-0.8 / 0.12-0.20
Snøhvit-Tub (mean) [47,49]	3	0.33	38	
Quest (mean) [50]	3	0.58	66	0.1 / 0.17
Decatur (mean) [51,52]	1	0.33	38	0.185 / 0.20
In Salah (mean) [53,54]	18	0.21	24	0.01 / 0.18

Table A2. Injection rates and formation summary data from industrial-scale SAF storage projects in operation. Table updated with more recent data

	All wells	Offshore only
N=	60	34
Mean	0,532	0,695
Median	0,583	0,725
S.D.	0,271	0,222
1.645 times S.D.	0,446	0,364
P90 rate	0,086	0,330
P10 rate	0,978	1,059

Table A3. Statistics of injection rate data for all wells and for offshore projects only (P90 and P10 give the 90% confidence interval)

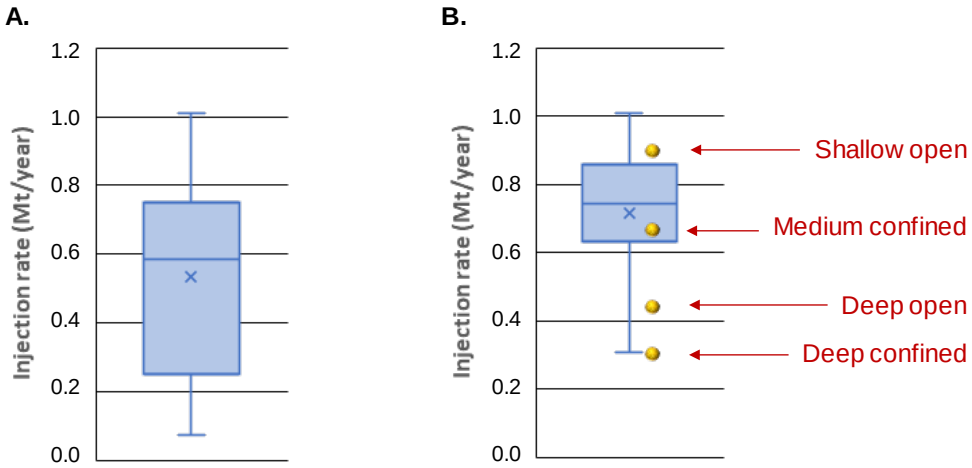

Figure A7. (A) Box and whisker plots of rate distributions data from all storage projects in operation and (B) Similar plot for offshore wells compared with mean rates for model scenarios (yellow symbols).

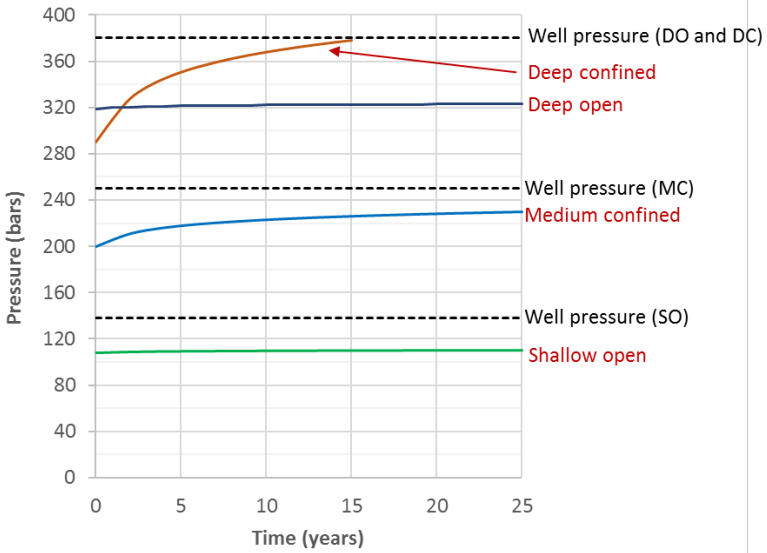

Figure A8. Pressure functions for modelled scenarios (coloured lines are reservoir pressure; dotted lines are well pressure, BHP).

A5 Growth curve for GCS injection wells – methods and uncertainties

All new technologies experience an early steep growth curve, typically exponential growth for decades, until they become routine. GCS is at the beginning of that growth curve[55]. This early period is one of rapid innovation and cost reduction and development of economies of scale. This concept of technology market penetration and commercial materiality has been well studied for different technologies, with one recent analysis comparing anticipated CCS development with historic industrial deployment examples[56]. Given a current global CO_2 storage rate of <10 Mt CO_2 storage per year and an anticipated future rate of a few Gtpa by 2050, a scale up of >2 orders of magnitude over decades is required. This is not dissimilar from the historic performance of other technologies and can be considered as a reasonable initial expectation given a favorable economic environment, which admittedly has yet to fully mature (although successful tax and credit trading schemes are emerging and being implemented in some regions).

A useful perspective for evaluating realistic CCS deployment timelines is to look at historic hydrocarbon development. While some aspects of CCS deployment may differ from hydrocarbon extraction, sufficient experience with large-scale hydrocarbon resource development exists to anticipate the pace of CCS injection well deployment. In many ways, the similarities of the two activities and decades of prior experience suggest CCS could likely improve on early hydrocarbon industry rates of well deployment, although that is only speculation, so we take prior technical and temporal development experience as a minimum bound on CO_2 injection well deployment rate. The subsequent analysis assumes economic viability (costs are not considered, but favorable economics are recognized as required to drive CCS activity), and no additional technological or engineering developments are considered (existing project technology considered sufficient, a very conservative assumption). The analysis simply uses historic well deployment data and injection rates anticipated based on current experience to confirm CCS viability on the needed decadal timeline already established.

These curves exhibit a characteristic shape related to their hydrocarbon extraction context, which relates to basin hydrocarbon 'creaming' curves[57,58,59]. The different maximum plateau values relate to overall basin size, total hydrocarbon resource retained, and degree of petroleum exploration. It is unknown if long-term CCS will emulate this overall temporal or spatial evolution of hydrocarbon development, but considerations of regional pressure presented in the main paper are consistent with creaming concepts, as the pressure resource of an area is likely to be exhausted before the total available rock pore volume is.

We have used historic well data to speculate on what the development of offshore CCS could look like in the future (Main paper[11], Fig. 6). The more granular and relatively small-scale example of historic well deployment for hydrocarbon extraction in the inner shelf of the Texas portion of the Gulf of Mexico (<10.5 miles offshore) may be most appropriate for considering initial short-term CCS development in a region. Offshore well drilling activity began in this region in approximately 1950 and about 1,800 total wells were drilled in around 60 years. This can be considered representative of an aggressive industrial development setting on a continental margin, but not atypical in a global sense in terms of aerial extent, water depth, or geology, and is the most conservative well development model for CCS deployment (compared with the well data for the larger areas of the Norwegian North Sea and the US Gulf of Mexico).

Table A4 shows selected well-development scenarios based on the three historic datasets, used to illustrate the range in well rates and corresponding storage volumes achieved by 2050. Using the three regional and incrementally larger well-development models (Texas, Norway, GoM), a constant average well injection rate is applied to the well development timeline to calculate the incremental and cumulative CO_2 stored. The 'Texas model' results indicate that global goals are not achieved in any scenario (varying injection rate and/or number of wells). Unrealistically high individual well rates (>4 Mtpa) would be needed to achieve total injection rates of 7 Gtpa in 2050. The Norwegian model results are more promising, in that five 'Norway region' models could achieve the goal of 7 Gtpa in 2050, assuming realistic average injection rates 0.67 Mtpa for 10,415 wells. The 'Gulf of Mexico' model

results represent the most aggressive development case considered. Reasonable individual well injection rates allow the goal of 7 Gtpa in 2050 to be exceeded and could exceed 100 Gt cumulative storage. Of course, it is unlikely that one region will develop this aggressively to achieve needed reductions by itself.

2020+ Scenario	Offshore Well model	Number of regions	Avg. Well Inj. Rate (Mt/yr)	# active wells in 2050	Incremental Rate in 2050 (Mt/yr)	Cumulative Mass in 2050 (Mt CO_2)	Comment
A	Texas	1	0.7*	345	242	1,781	Goals not met
B	Texas	5	0.7*	1,725	1,208	8,904	Goals not met
C	Texas	5	4.058	1,725	7,000*	51,617	Incremental rate goals met, but not cumulative; injection rate high
D	Norway	1	0.7	2,083	1,458	15,243	Goals not met
E	Norway	1	3.36	2,083	7,000*	73,164	Incremental rate goals met, but not cumulative; injection rate very high
F	Norway	**5**	**0.672**	**10,415**	**7,000***	**73,164**	**Most plausible**
G	GoM	1	0.7*	17,155	12,009	116,523	Unlikely one region will develop this aggressively; Incremental goal exceeded; Close to cumulative goal
H	GoM	1	0.408	17,155	7,000*	67,916	Injection rate low, not cost effective; Cumulative goal not met

Table A4: Eight possible scenarios for CCS development on continental shelves based on historic examples of hydrocarbon well development from three different offshore regions: Texas, Norway, and Gulf of Mexico (GoM). Each scenario uses one of 3 historically-based models for well development (Main paper Fig. 6) and considers constant average individual well injection rates and three metrics for the year 2050: the total number of active wells (based on historical development, modified for 25-year lifespan), the total rate of CO_2 injection at that time, and the cumulative mass of CO_2 injected. Values with an asterisk are prescribed in each scenario, with the others being dependent values. Column 6 is the product of values in columns 4 and 5. Scenario F seems most plausible for giga-ton scale deployment, requiring a well development model similar to historic Norwegian hydrocarbon exploitation to be applied for CCS in 5-7 regions globally, with a reasonable mean well injection rate of approximately 0.67 Mt/yr.

For an additional perspective on a fully mature global injection scenario, from 1968 to 2001 (33 years), there were globally on average around 1,500 new hydrocarbon exploration wells drilled per year outside of the US and Canada in all water depths, with a peak of around 2,200 and a low of 800 per year[60]. Globally, 17,700 wells were drilled in shallow water since 1940 (similar to Scenario G, Table A4). This represents a mature global hydrocarbon development stage, so is arguably similar to what mature GCS could achieve eventually. Not all of those wells were successful (encountered economic hydrocarbons), so a failure rate may need to be considered. However, given the current maturity of basin knowledge, new CO_2 storage injectors should have a high success rate. Assuming (for a CCS scenario) that each of the projected 1,500 wells per year achieves an average injection rate of 0.5 Mt/yr (allowing for many unsuccessful wells), this equates to increasing global CO_2 storage by 750 Mt/yr each year. The cumulative storage of this mature activity over a decade (from say 2050 to 2060) would be to store over 40 Gt of CO_2. Clearly this would require development of a global CCS industry comparable to the size of the hydrocarbon exploration industry in about half the time. Challenging, but credible. Such industrial growth could drive investment, employment, and long-term prosperity in many regions, but would need to be accompanied by favorable economic markets/incentives such as globally validated and tradable CO_2 credits.

References (Appendix)

1. Haq, B.U., Hardenbol, J., & Vail, P.R. Chronology of Fluctuating Sea Levels Since the Triassic, *Science*: Vol. 235 (4793), 1156-1167 DOI: 10.1126/science.235.4793.1156 (1987).
2. Vail, P.R. Seismic Stratigraphy Interpretation Using Sequence Stratigraphy: Part 1: Seismic Stratigraphy Interpretation Procedure, In: A. W. Bally (Ed.) *AAPG Studies in Geology #27*, volume 1: Atlas of Seismic Stratigraphy (1987).
3. Van Wagoner, J.C., H.W. Posamentier, R.M. Mitchum, P.R. Vail, J.F. Sarg, T.S. Loutit, and J. Hardenbol. An overview of the fundamentals of sequence stratigraphy and key definitions, SEP Special Publication No. 42, The Society of Economic Paleontologists and Mineralogists (1988).
4. Weeks L.G. Petroleum Resources Potential of Continental Margins, In: Burk C.A., Drake C.L. (eds) *The Geology of Continental Margins.* Springer, Berlin, Heidelberg (1974).
5. Magoon, L.B., and W.G. Dow, The petroleum system, in, Magoon, L.B., and W.G. Dow, eds, The Petroleum System-from Source to Trap: *AAPG Memoir 60*, p. 3-24 (1994)
6. Bolås, H. M. N., & Hermanrud, C. Hydrocarbon leakage processes and trap retention capacities offshore Norway. *Petroleum Geoscience,* 9(4), 321-332 (2003).
7. Osborne, M. J., & Swarbrick, R. E. Mechanisms for generating overpressure in sedimentary basins: A reevaluation. *AAPG bulletin,* 81(6), 1023-1041 (1997).
8. Schowalter, T.T. Mechanics of secondary hydrocarbon migration and entrapment, *AAPG Bulletin,* 63(5): 723-760 (1979).
9. Demaison, G. & Huizinga, B.J. Genetic classification of petroleum systems, *AAPG Bulletin,* 75(10): 1626-1643 (1991).
10. Zoback, M.L. First- and second-order patterns of stress in the lithosphere: The World Stress Map Project, *JGR Solid Earth,* V97(B8): 11703-11728, https://doi.org/10.1029/92JB00132 (1992)
11. Ringrose, P.S. & Meckel, T.A. Maturing global CO2 storage resources on offshore continental margins to achieve 2DS emissions reductions (this submission, 2019).
12. Grollimund, B. & Zoback, M.D. Impact of glacially-induced stress changes on fault seal integrity offshore Norway, *AAPG Bulletin*, 87(3): 493-506 (2003).
13. Plaza-Faverola, A., Buenz, S. Mienert, J. Repeated fluid expulsion through sub-seabed chimneys offshore Norway in response to glacial cycles, *Earth and Planetary Science Letters,* 305: 297-308 (2011).
14. Longley, I.M., C. Buessenschuett, L. Clydsdale, C.J. Cubitt, C.J., Davis, R.C., Johnson, M.K., Marshall, N.M., Murray, A.P., Somerville, R., Spry, T.B and N.B. Thompson, 2003, The North West Shelf of Australia – A Woodside Perspective, AAPG Search and Discovery article #10041.
15. Xie, F., Q. Wu, L. Wang, Z. Shi, C. Zhang, B. Liu, C. Wang, Z. Shu, and H. Di, 2017, Passive continental margin basins and the controls on the formation of evaporates: a case study of the Gulf of Mexico Basin, Carbonates Evaporites, DOI 10.1007/s13146-017-0404-z.
16. Mohriak, W.U., and S. Leroy, 2013, Architecture of rifted continental margins and break-up evolution: insights from the South Atlantic, North Atlantic and Red Sea-Gulf of Aden conjugate margins, In: Mohriak, W. U., Danforth, A., Post, P. J., Brown, D. E., Tari, G. C., Nemcˇok, M.&Sinha, S. T. (eds) 2013. Conjugate Divergent Margins. Geological Society, London, Special Publications, 369, 497–535.
17. Tang, L., J. Ren, K. Mcintosh, X. Pang, C. Lei, and Y. Zhao, 2018, The structure and evolution of deepwater basins in the distal margin of the northern South China Sea and their implications for the formation of the continental margin, Marine and Petroleum Geology, 92: 234-254, https://doi.org/10.1016/j.marpetgeo.2018.02.032
18. Nooner, S. L., Eiken, O., Hermanrud, C., Sasagawa, G. S., Stenvold, T., & Zumberge, M. A. Constraints on the *in situ* density of CO2 within the Utsira formation from time-lapse seafloor gravity measurements. *International Journal of Greenhouse Gas Control,* 1(2), 198-214 (2007).
19. Turner R.E., Rabalais N.N. & Justić D. Trends in summer bottom-water temperatures on the northern Gulf of Mexico continental shelf from 1985 to 2015. *PLoS ONE* 12(9): e0184350. https://doi.org/10.1371/journal.pone.0184350 (2017).
20. Singh, V. P., Cavanagh, A., Hansen, H., Nazarian, B., Iding, M., & Ringrose, P. S. Reservoir modeling of CO2 plume behavior calibrated against monitoring data from Sleipner, Norway. In SPE annual technical conference and exhibition. *Society of Petroleum Engineers (*2010).
21. Meckel, T.A., Nicholson A.J. & Treviño, R.H. Capillary aspects of fault-seal capacity for CO_2 storage, Lower Miocene, Texas Gulf of Mexico, In: Treviño, R.H., and T.A. Meckel, Eds., Geological CO_2 sequestration atlas of Miocene strata, offshore Texas state waters, Bureau of Economic Geology, Report of Investigations No. 283 (The University of Texas at Austin, 2018).
22. Morris, S., B. Vestal, K. O'Neill, M. Moretti, C. Franco, N. Hitchings, J. Zhang, and J.D. Grace, The pore pressure regime of the northern Gulf of Mexico: Geostatistical estimation and regional controls, *AAPG Bulletin,* 99(1): 91-118 (2015).
23. Yang, C., R.H. Trevino, T. Zhang, K.D. Romanak, K. Wallace, J. Lu, P.J. Mickler, & S.D. Hovorka, Regional assessment of CO_2-solubility trapping potential: A case study of the coastal and offshore Texas Miocene interval, *Environmental Science and Technology,* 48: 8275-8282, dx.doi.org/10.1021/es502152y (2014).
24. U.S. Geological Survey World Petroleum Assessment 2000, Digital Data Series 60, https://energy.usgs.gov/OilGas/AssessmentsData/WorldPetroleumAssessment.aspx (2000)
25. Eaton, B.A. Fracture gradient prediction and its application in oilfield operations, Society of Petroleum Engineers, SPE-2163-PA, https://doi.org/10.2118/2163-PA (1969).

26. Marbun, B.T.H., A.N. Corina, G.V. Arimbawa, R. Aristya, S. Purwito, and A.F. Hardama, A new approaching method to estimate fracture gradient by correcting Matthew-Kelley and Eaton's stress ratio, *Journal of Petroleum Science and Engineering,* 135: 261-267 (2015).
27. Treviño, R.H., & T.A. Meckel (Eds.) Geological CO_2 sequestration atlas of Miocene strata, offshore Texas state waters, Bureau of Economic Geology, Report of Investigations No. 283, The University of Texas at Austin, 74 p. (2017).
28. Vangkilde-Pedersen, T., Anthonsen, K. L., Smith, N., Kirk, K., Neele, F., van der Meer, B., ... & Hendriks, C. Assessing European capacity for geological storage of carbon dioxide–the EU GeoCapacity project. *Energy Procedia,* 1(1), 2663-2670 (2009).
29. Bentham, M., Mallows, T., Lowndes, J., & Green, A. CO2 Storage Evaluation Database (CO2 Stored): the UK's online storage atlas. *Energy Procedia,* 63, 5103-5113 (2014).
30. Halland, E. K., Mujezinovic, J., & Riis, F. CO_2 Storage Atlas: Norwegian Continental Shelf, Norwegian Petroleum Directorate, PO Box 600, NO-4003 Stavanger, Norway, 2014. URL http://www.npd. no/en/Publications/Reports/Compiled-CO2-atlas (2014).
31. NETL, 2015. Carbon Storage Atlas, 5th Edn. https://www.netl.doe.gov/
32. Hendriks, C., and W. Graus, Global Carbon Dioxide Storage Potential and Costs, In: EEP-02001 Ecofys (2004).
33. Metz, B., Davidson, O., De Coninck, H., Loos, M. and Meyer, L. *Carbon dioxide capture and storage:* Working Group III of the Intergovernmental Panel on Climate Change. Cambridge, United Kingdom and New York, NY, USA 442 (2005).
34. Dooley, J.J., Estimating the supply and demand for deep geologic CO_2 storage capacity over the course of the 21st century: A meta-analysis of the literature, *Energy Procedia*, *37*, 5141-5150 (2013).
35. Gorecki, C. D., Sorensen, J. A., Bremer, J. M., Knudsen, D., Smith, S. A., Steadman, E. N., & Harju, J. A. Development of storage coefficients for determining the effective CO_2 storage resource in deep saline formations. In SPE International Conference on CO2 Capture, Storage, and Utilization. Society of Petroleum Engineers (2009).
36. Nordbotten, J. M., & Celia, M. A. Similarity solutions for fluid injection into confined aquifers. *Journal of Fluid Mechanics,* 561, 307-327 (2006).
37. Okwen, R. T., Stewart, M. T., & Cunningham, J. A. Analytical solution for estimating storage efficiency of geologic sequestration of CO2. *International Journal of Greenhouse Gas Control,* 4(1), 102-107 (2010).
38. Ringrose, P. S., The CCS hub in Norway: some insights from 22 years of saline aquifer storage. *Energy Procedia,* 146, 166-172 (2018).
39. Zoback, M.D. Reservoir Geomechanics. Cambridge University Press, Cambridge, UK (2007).
40. Bohloli, B., Ringrose, P., Grande, L., & Nazarian, B. Determination of the fracture pressure from CO2 injection time-series datasets. *International Journal of Greenhouse Gas Control,* 61, 85-93 (2017).
41. Zhang, J. Pore pressure prediction from well logs: Methods, modifications, and new approaches. *Earth-Science Reviews,* 108(1-2), 50-63 (2011).
42. Golan, M., & Whitson, C. H. Well performance (p. 469). Englewood Cliffs, New Jersey: Prentice Hall (1991).
43. Ringrose, P., Greenberg, S., Whittaker, S., Nazarian, B., & Oye, V. Building confidence in CO2 storage using reference datasets from demonstration projects. *Energy Procedia,* 114, 3547-3557 (2017).
44. Pawar, R. J., Bromhal, G. S., Carey, J. W., Foxall, W., Korre, A., Ringrose, P. S., ... & White, J. A. Recent advances in risk assessment and risk management of geologic CO 2 storage. *International Journal of Greenhouse Gas Control,* 40, 292-311 (2015).
45. Miller, C. C., Dyes, A. B., & Hutchinson Jr, C. A. The estimation of permeability and reservoir pressure from bottom hole pressure build-up characteristics. *Journal of Petroleum Technology*, *2*(04), 91-104 (1950).
46. Dake, L. P. The practice of reservoir engineering. *Developments in petroleum science*, 36, 311-458 (1994).
47. Hansen, O., Gilding, D., Nazarian, B., Osdal, B., Ringrose, P., Kristoffersen, J. B., ... & Hansen, H. Snøhvit: The history of injecting and storing 1 Mt CO2 in the fluvial Tubåen Fm. *Energy Procedia,* 37, 3565-3573 (2013).
48. Maldal, T., & Tappel, I. M. CO_2 underground storage for Snøhvit gas field development. *Energy,* 29(9-10), 1403-1411 (2004).
49. Eiken, O., Ringrose, P., Hermanrud, C., Nazarian, B., Torp, T. A., & Høier, L. Lessons learned from 14 years of CCS operations: Sleipner, In Salah and Snøhvit. *Energy Procedia,* 4, 5541-5548 (2011).
50. Rock, L., O'Brien, S., Tessarolo, S., Duer, J., Bacci, V. O., Hirst, B., ... & Halladay, A. The Quest CCS Project: 1st Year Review Post Start of Injection. *Energy Procedia*, *114*, 5320-5328 (2017).
51. Finley, R. J., Frailey, S. M., Leetaru, H. E., Senel, O., Couëslan, M. L., & Scott, M. Early operational experience at a one-million tonne CCS demonstration project, Decatur, Illinois, USA. *Energy Procedia*, *37*, 6149-6155 (2013).
52. Gollakota, S., & McDonald, S. Commercial-scale CCS project in Decatur, Illinois–construction status and operational plans for demonstration. *Energy Procedia*, *63*, 5986-5993 (2014).
53. Wright, I. W., Ringrose, P. S., Mathieson, A. S., & Eiken, O. An overview of active large-scale CO2 storage projects. In SPE International Conference on CO2 Capture, Storage, and Utilization. Society of Petroleum Engineers (2009).
54. Ringrose, P. S., Mathieson, A. S., Wright, I. W., Selama, F., Hansen, O., Bissell, R., ... & Midgley, J. The In Salah CO2 storage project: lessons learned and knowledge transfer. *Energy Procedia,* 37, 6226-6236 (2013).
55. Reiner, D.M., Learning through a portfolio of carbon capture and storage demonstration projects, *Nature Energy* Vol. 1, Article number: 15011 (2016).
56. Kramer, G.J. & Haigh, M. No quick switch to low-carbon energy, *Nature* 462: 568–569 (2009) [their Fig. 1]
57. Arps, J.J. & Roberts, T.G. Economics of drilling for Cretaceous oil on the east flank of the Denver-Julesburg Basin, *American Association of Petroleum Geologists Bulletin,* v. 42, no. 11, p. 2549-2566 (1958).

58. Meisner, J. & Demirmen, F. The creaming method: a bayesian procedure to forecast future oil and gas discoveries in mature exploration provinces: *Journal of the Royal Statistical Society*, v. 144, part A, p. 1-31 (1981).
59. Drew, LJ., and Lore, G.L, Field growth in the Gulf of Mexico--A progress report, in USGS Research on Energy Resources, 1992: *U.S. Geological Survey Circular 1074,* p. 22-23 (1992).
60. Attanasi, E.D., Freeman, P.A. & Glovier, J.A. Statistics of Petroleum Exploration in the World Outside the United States and Canada Through 2001, *USGS Circular 1288 (*2007).